THE JOURNAL OF COMPARATIVE NEUROLOGY 320:415–434 (1992)

Visuotopic Organization of Corticocortical Connections in the Visual System of the Cat

P.A. SALIN, P. GIRARD, H. KENNEDY, AND J. BULLIER
Vision et Motricité, INSERM 94, 69500 Bron, France

ABSTRACT

It has recently been demonstrated that, in contrast with the retinogeniculocortical projection, the corticocortical connections in the cat present a high degree of convergence and divergence. This suggests that some corticocortical connections link nonvisuotopically corresponding regions. Using fine-grain electrophysiological mapping and anatomical tracing, we have set out to test this possibility by placing a small injection of retrograde tracer in area 17 and by comparing the extent of visual field encoded in the region of area 18 containing labeled cells and that represented in the uptake zone.

The results demonstrate that the size of the labeled region on the surface of area 18 is independent of eccentricity and that, despite its anisotrophy, this region of labeling encodes a broadly circular region of visual field that is larger than that encoded in the uptake zone of the tracer in area 17. For example, in the representation of lower visual field, a virtual point in area 17 that encodes a visual field region 4° in diameter receives afferents from a region of area 18 encoding a region 11° wide. Examination of the density of labeled cells in the labeled zone in area 18 reveals that the highest density is observed in a region in visuotopic correspondence with the injection site. However, high labeling density is also occasionally found in patches that do not represent the same visual field region as the injection site. Many receptive fields of neurons recorded in the labeled zone in area 18 only partially overlap or fail to overlap the visual field region encoded by the injection site.

The results also demonstrate that the extent of visual field encoded in the labeled zone in area 18 is the same as that represented in the region of intrinsic labeling in area 17. It is suggested that cortical afferents coming from several cortical areas and converging on a column of cells in area 17 cover the same extent of visual field and that this cortical network constitutes the structural basis for the modulatory regions of the receptive field as well as the synchronization of neurons in different cortical areas.

Key words: electrophysiological mapping, convergence, areas 17 and 18, receptive field overlap, nonvisuotopic connections, retrograde tracers

It is commonly believed that a neuron's receptive field (RF) is a functional manifestation of its anatomical input (Jacobs, '69). This would lead one to predict that the RF of a neuron encompasses the sensory field encoded by the neurons afferent to it. In the visual system, this sort of organization we will refer to as strictly visuotopic; it has been shown to be the dominant feature of retinogeniculate and geniculostriate pathways (Cleland et al., '71; Tanaka, '83). Interestingly, a strict visuotopic organization has also been reported in descending cortical pathways (McIlwain, '73, '77). However, there is indirect evidence that corticocortical connections are not organized according to a strict visuotopic principle as is the case at the subcortical level. For instance, given the length of intrinsic connections, it is likely that they can link cortical regions containing neurons that do not have overlapping receptive fields (Gilbert, '85; Gilbert and Wiesel, '89; Luhmann et al., '90). The most extensive evidence for a mismatch in the RFs of interconnected cortical regions comes from work on callosal pathways. Here, combined anatomical and electrophysiological studies have shown, both in visual and somatosensory pathways, that interhemispheric pathways connect cortical regions that do not encode a common region of the sensory periphery (see Kennedy et al., '91 for a review).

A departure from a strict visuotopic organization is not necessarily all or nothing. It is possible that neurons

Accepted February 7, 1992.

Address correspondence and reprint requests to Dr. J. Bullier, INSERM 94, 16, Avenue du Doyen Lépine 69500 Bron, France.

respond to stimulation of part of the visual space encoded by their afferents. In this case the RFs of target and source neurons will show partial overlap and we will refer to such connections as partially visuotopic. Alternatively, source and target neurons can have completely separate RFs. Such connections we refer to as nonvisuotopic.

To date, the idea that corticocortical association pathways might not fulfill the criteria of strict visuotopy stems mainly from anatomical studies. In the visual cortex, neurons labeled by an injection of retrograde tracer in a given area occupy a very large extent of cortex in other visual areas (Gilbert and Kelly, '75; Bullier et al., '84b; Symonds and Rosenquist, '84; Kennedy and Bullier, '85; Gilbert and Wiesel, '89). In contrast, the same injections give localized populations of labeled neurons in the dorsal lateral geniculate nucleus (LGN) (Geisert, '80; Bullier et al., '84a; Kennedy and Bullier, '85; Perkel et al., '86) or in the retina after small LGN injections (Illing and Wassle, '81). Thus, corticocortical projections appear to present a different geometrical organization from retinogeniculate and geniculostriate connections.

Recently, we have developed a method to quantify two projection parameters: convergence (the extent of a source structure projecting to a virtual point in a target structure) and divergence (the extent of the target innervated by a virtual point in the source structure) (Salin et al., '89). Using this method, we have been able to calculate the divergence and convergence of projections to area 17 in the cat (Salin et al., '89). In that study we showed that a virtual point in area 17 is innervated by a region in area 18 measuring 4.9 mm in the caudorostral axis. When this convergence value is considered in conjunction with published maps of the representation of visual space in area 18, it appears that the projection from area 18 to area 17 does not conform to a strict visuotopic organization.

In order to characterize the geometry of the visual field region represented by the neurons in area 18 sending projections to a small region of area 17, we have undertaken a direct study of the visuotopic organization of the projections between areas 18 and 17. Although ideally one would like to characterize the receptive fields of interconnected neurons in different areas, this is technically difficult if not impossible. Instead, what we have undertaken is to determine the visual field represented in interconnected regions in areas 17 and 18 by combining electrophysiological mapping and neuroanatomical tracing. To this end, in the present study we have placed small injections of retrograde tracers in the target area (area 17) and established a fine grain map of visual space in the source (area 18) and target areas. This has enabled us to measure directly the extent of visual space represented in the region of area 18 containing labeled neurons and compare it to the extent of visual space represented in the uptake zone of the tracer.

By combining physiological mapping of area 18 with injections of tracers in area 17, we first compared the sizes of the regions containing the receptive field centers of neurons in the zone of labeling in area 18 and in the uptake zone in area 17. We then compared the visual space covered by the receptive fields of the neurons in these two regions. By examining the results from injections placed at different eccentricities in area 17, we have been able to determine whether retinal eccentricity influences the size of the labeled zone and its representation of visual space. Finally, the question arises of whether regions of the labeled zone that do not correspond visuotopically to the injection site only contain scattered labeled cells or whether they correspond to high densities of labeled cells. Thus we have measured the labeled cell density fluctuations across the labeled zone and related it to the representation of visual space in this region.

MATERIALS AND METHODS

Surgery and anesthesia

Adult cats (2.8–4 kg) were initially anesthetized by an intramuscular injection of ketamine hydrochloride (Imalgène, 15 mg/kg) and of chlorpromazine (Largactil, 1 mg/kg). An intravenous catheter was placed in the cephalic vein, and an endotracheal tube was positioned. During surgery, the animals were anesthetized by repeated intravenous injections of 0.1 ml of alphadolone and alphaxolone (Saffan). During recording, they were paralyzed by a continuous infusion of gallamine triethiodide (Flaxedil, 10 mg/kg/h) and artificially ventilated with a mixture of N_2O/O_2 (70/30%). Additional anesthesia was provided by a continuous infusion of pentobarbital sodium (Nembutal, 1 mg/kg/h) or by adding 0.2–0.4% halothane (case PAS28). The end-tidal CO_2 level, the EEG, and the heart rate were monitored and maintained at proper levels. The nictitating membranes of both eyes were retracted and the pupils dilated by application of 5% phenylephrine and 0.5% atropine. Plano contact lenses of appropriate curvature were fitted to the corneal surface.

Electrophysiological recording

Prior to the first recording session in area 17, a craniotomy was made above the lateral sulcus. The dura matter was reflected from the region where area 17 is located. Tungsten-in-glass microelectrodes with impedances of 1–4 MΩ before plating (Merrill and Ainsworth, '72) were used to record single and multiple units. The excitatory discharge region of the receptive field was characterized with hand-held stimuli by plotting the minimal response field (Barlow et al., '67). Refractive lenses were used to focus the eyes at a distance of 1.14 m and Risley prisms to superimpose the visual axes of the two eyes while recording from a binocular cell. Throughout the session, the extent of eye movements was monitored by using the position on the tangent screen of a small receptive field of a neuron recorded by a second electrode in area 17 near the representation of the area centralis. RFs were located with respect to the area centralis, derived from the position of the blind spot (Nikara et al., '68) obtained by back-projection of the retina on the tangent screen. With this procedure, the position of the area centralis can be estimated with a precision that is of the order of 1° (Cooper and Pettigrew, '79). The positions of electrode penetrations were marked on a photograph of the cortical surface that focused on the small blood vessels.

After recording at several sites within area 17, diamidinoyellow (DY) (Keizer et al., '83), fast blue (FB) (Bentivoglio et al., '80), or rhodamine-filled latex microspheres (Rh, Lumafluor) (Katz et al., '84) were injected in area 17 by means of a micropipette sealed to a Hamilton syringe and with an aperture of 40–60 μm. Injections of 0.05–0.1 μl of 3% FB and DY and injections of 0.2 μl undiluted Rh were made at a depth of 400–700 μm with an angle larger than 60° to the pial surface. The location of the injection site was also marked on the photomicrograph of the cortical surface used for recording electrode penetrations. Injections in

rostral area 17 were made on the medial bank of the lateral gyrus. More caudally, injections in central area 17 were made on the dorsal surface of the cortex, next to the interhemispheric fissure. At the end of the recording session, Flaxedil was discontinued and Nembutal replaced by repeated doses of Saffan. Prophylactic intramuscular injection of an antibiotic and of dexamethasone (Soludecadron 4 mg) were made and the cat was replaced in its home cage after it had recovered.

Eleven days later, animals were prepared for a second recording session. A rectangular region (10 × 6 mm) of area 18 situated lateral to the injection sites was mapped during a session lasting 24–48 hours. After removing the dura matter, a circular cylinder was placed around the craniotomy and filled with silicon oil. For recordings on the lateral gyrus, electrode penetrations were separated on average by 1 mm in the caudal direction and by 0.5 mm in the mediolateral direction. During each penetration, receptive field positions were determined for one or several neurons situated at a depth of 200–900 μm. Approximately 30 penetrations and 15 electrolytic lesions (10 μA during 10 seconds) were made in each animal. More than half the penetrations were marked with lesions and penetrations with no lesions were within 0.5 mm of penetrations with lesions. In order to align successive sections cut tangentially to the surface of the physically flattened brain, it was necessary for lesions to span the entire thickness of cortex. This was ensured by two lesions being made at two different depths (350–450 μm and 750–850 μm). For those penetrations in the bank of the lateral sulcus that spanned long distances in the cortex, each penetration contained several lesions.

The match of the RFs recorded during the two sessions was made by using the position of the blind spot and the pattern of retinal blood vessels reflected on the tangent screen. In two cases (PAS16 and PAS28), the injections of the dyes and the mapping of area 17 were carried out during the same session as the mapping of area 18.

Histological procedures

At the end of the second electrophysiological mapping session, the cat received a lethal dose of sodium pentobarbital and was perfused through the heart with saline, followed in those animals in which the cortex was physically flattened by 2% paraformaldehyde in phosphate buffer for 5 minutes and then by a mixture of 2% paraformaldehyde and 10% sucrose for 5 minutes (personal communication of Lea Krubitzer; Olavarria and Van Sluyters, '85). The cortex was removed and flattened between glass plates for 12 hours in a solution of 10% paraformaldehyde and 30% sucrose. Frozen sections (40 μm) were cut parallel to the pial surface. This procedure usually gives a low degree of distortion (inferior to 5%) (Olavarria and Van Sluyters, '85; Tootell and Silverman, '85; Freeman et al., '87). The coefficient of shrinkage calculated for this flattening procedure is equal to 0.96.

Several sections were reacted for cytochrome oxidase activity (Wong-Riley, '79a; Price, '85) and others for myelinated fibers (Gallyas, '79). Cytochrome oxidase- and myelin-stained sections were used for determining the border between areas 18 and 19. In cases PAS11 and PAS14, the A17/A18 border determined on myelin-stained sections corresponded accurately to the border estimated from the electrophysiological mapping. Parasagittal or coronal sections of the thalamus containing the LGN were cut and counterstained with cresyl violet.

For PAS16 and PAS28, electrode penetrations were placed near the representation of the area centralis, in a region of high degree of curvature of area 18. Previous results have shown that physically flattening the cortex in those conditions would lead to large distortions due to cracking of the gray matter. Hence, in these cases, the cats were perfused by a classical procedure for the fluorescent dyes described in a previous article (Bullier et al., '84a). In PAS16, two-dimensional reconstructions of the cortex were made from parasagittal sections separated by 480 μm according to the method of Van Essen and Maunsell ('80). In PAS28, a two-dimensional reconstruction of the cortex was made from coronal sections separated by 240 μm. The surface calculations presented in the results are corrected by the shrinkage coefficient, which is equal to 0.9 for PAS16 and 0.84 for PAS28. Histological sections were counterstained by cresyl violet and stained for myelin so as to reveal the A17/A18 and the A18/A19 borders (Sanides and Hoffmann, '69).

Sections were briefly dehydrated and mounted in Fluoromount, which improves the visibility of the labeling. They were examined at a magnification of 400 or 1,000 under UV illumination with oil-immersion objectives and a Leitz fluorescence microscope equipped with two filters, one for DY and FB (Filter D: 355–425 nm) and another for Rh (filter: 510–560 nm). Plots of retrogradely labeled cells were made with an X-Y plotter electronically coupled to the microscope stage. The counts of labeled cells in area 18 were made within a square grid of 480 × 480 μm for all cases, except for PAS28 where the size of the grid was 240 × 240 μm. Counts of labeled neurons were used to determine fluctuations of cell density across the cortical surface by using a surface interpolation of cell densities sampled at regular intervals on the flattened cortex. Graphs were constructed by using a Deltagraph R 1.0 Macintosh software package (cubic spline interpolation). In PAS11, the average density was computed on four sections situated in supragranular layers and for PAS16 and PAS28, the density of labeled cells was calculated in supra- and in infragranular layers from one in six sections. The precise alignment of plots of successive tangential sections was carried out with the electrolytic lesions and the sites of fluorescent tracers. Additional landmarks were provided by small injections of vital dyes (alcian blue and neutral red) and pinholes made on the frozen block during sectioning. The registration between the plots of labeled cells and the electrophysiological mapping was carried out by using the positions where the electrolytic lesions were made as recorded on the photographic view of the cortex. Areas of labeling on the flattened cortex and the visual field that

TABLE 1. Experimental Cases—Surface Areas of Cortex in Uptake and Labeled Zones and of Their Aggregate RFs

		Uptake zone		Labeled zone	
Case	Dye	Surface (mm^2)	AGG RF (deg^2)	Surface (mm^2)	AGG RF (deg^2)
PAS8	DY Az:1.3°, El:−11°	1.04	26.6	15	170
	FB Az:1.1°, El:−13°	0.58	24.2	9.8	142
PAS11	DY Az:3.1°, El:−12°	0.77	23.9	12.5	165
	FB Az:4.9°, El:−16.1°	0.94	30.4	9	150
PAS14	DY Az:7.5°, El:−11°	1.55	31.7	10.9	220
PAS16	DY Az:2.2°, El:−1.1°	0.45	5.3	10.5	38
	RH Az:2.3°, El:−0.5°	0.51	5.6	9.5	29
PAS28	FB Az:2.1°, El:−2.3°	0.45	5.7	12.2	59

Az, azimuth; El, elevation; AGG RF, area of aggregate receptive field (RF) of uptake zone in area 17 or labeled zone in area 18 (see text); DY, diamino-yellow; FB, fast blue; RH, rhodamine beads.

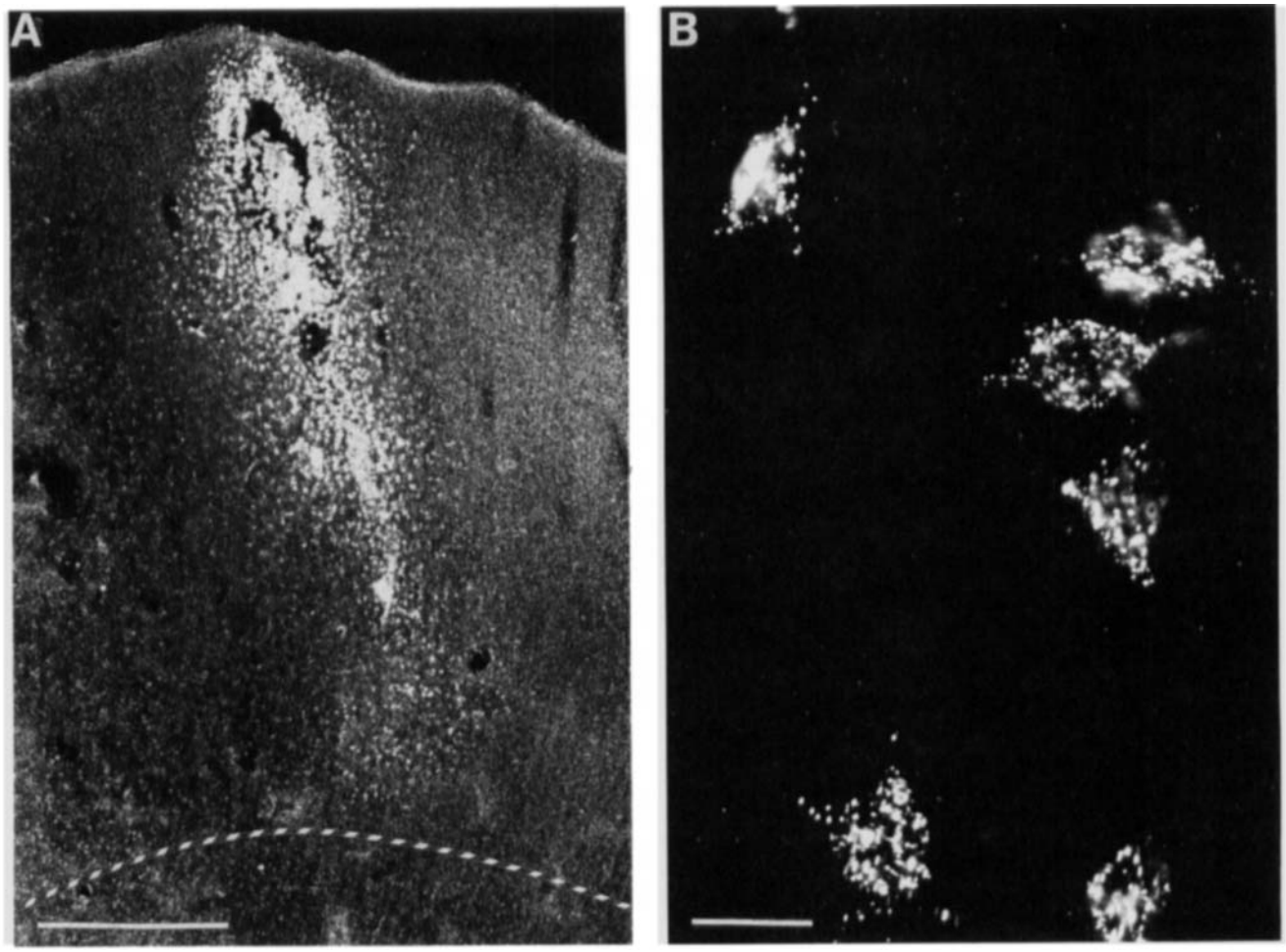

Fig. 1. Photomicrographs of an injection site of rhodamine-labeled latex microspheres in area 17 (**A**) and of retrogradely labeled neurons in area 18 (**B**). Interrupted line in A indicates the border between the gray and white matter. Case PAS16. Scale bar in A = 400 μm and in B = 30 μm.

they represent were measured by means of a digitizing tablet interfaced with an IBM PC.

RESULTS

Seven cats were used in these experiments. Injections of fluorescent tracers were made in the gray matter of area 17 so as to label neurons in area 18. After an appropriate survival period, the visual field was mapped in the region where labeling was expected. In five of the seven animals the following three criteria required to warrant description in the present report were met (Table 1). First, injections were successfully limited to the gray matter (Fig. 1A) and led to strong retrograde labeling, as shown in Figure 1B. Second, it was found that electrode penetrations had effectively explored a major portion of the labeled zone in area 18. Third, the injection sites were sufficiently far from the area 17/18 border to ensure that the uptake zone was restricted to area 17.

Configuration and extent of labeled zones across the cortex

The uptake region of rhodamine-labeled latex microspheres was taken as the region containing label near the injection site (Fig. 1A; Katz et al., '84; Cornwall and Philippson, '88). In the case of fluorescent tracers DY and FB, there is ample evidence that the region of dense extracellular coloration surrounding the needle track provides an *upper* estimate of the uptake zone (Keizer et al., '83; Bullier et al., '84a; Kennedy and Bullier, '85; Condé, '87; Ferrer et al., '88; see photomicrographs in Morel and Bullier, '90 and Dreher et al., '90).

In all cases, injections led to widespread labeling in the cortex and restricted labeling in the LGN. This is illustrated in Figure 2A where the areal extent of labeling using the physically flattened cortex (see Materials and Methods) is compared with the pattern of thalamic labeling (Fig. 2B). In this figure, the areal extent of the labeled zone has been determined by combining the labeling from several superimposed sections taken from different levels of the cortex combining all layers. The boundaries between cortical areas (dashed lines) were determined by myelin-stained sections as well as from the positions of RFs recorded in the electrode penetrations (in the case of the A17/A18 border).

Both injections in area 17 had small uptake zones, which are shown in black in Figure 2A. In the LGN, FB-, and DY-labeled neurons form two columns some 0.4 mm in

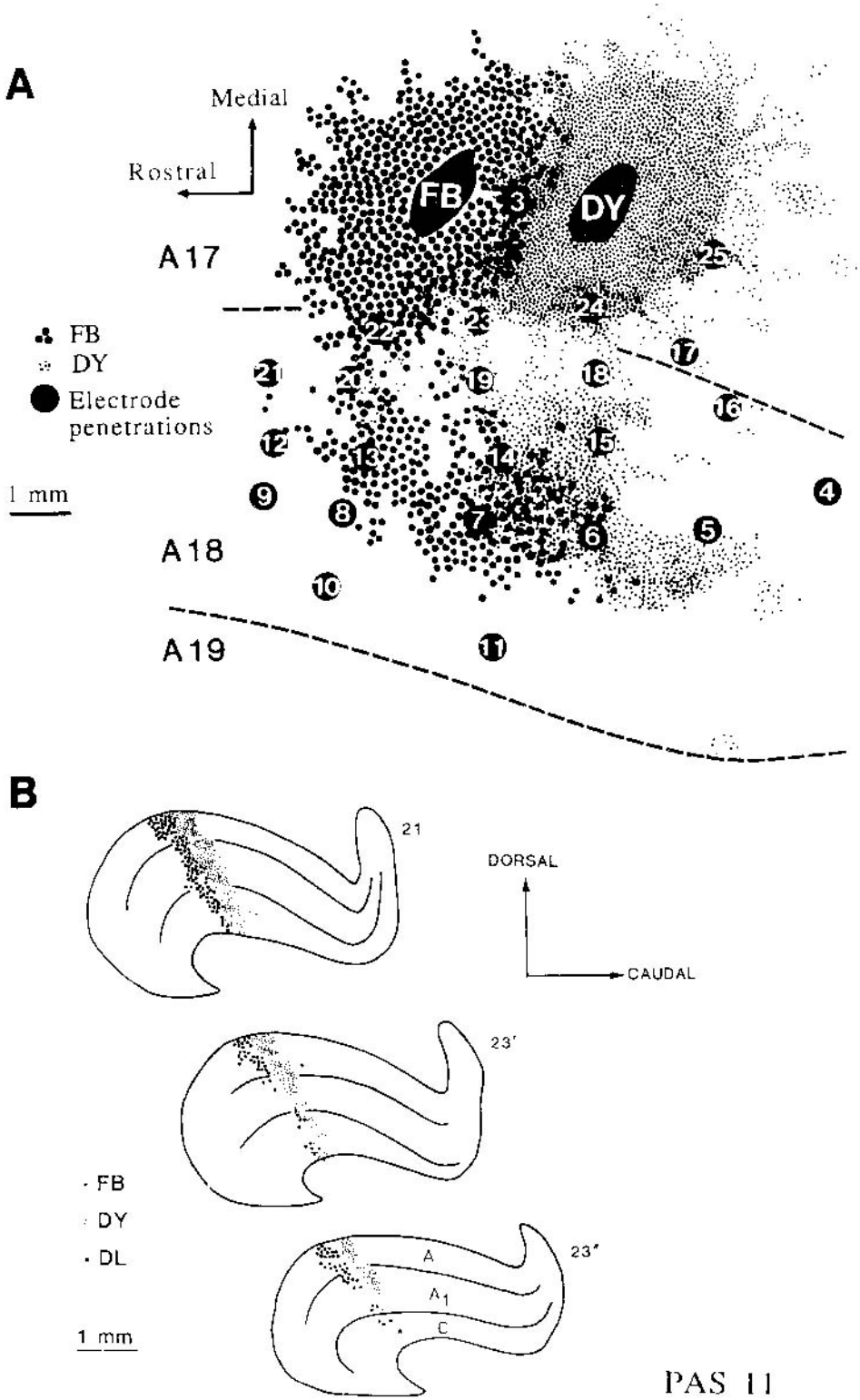

Fig. 2. Distribution of DY- and FB-labeled neurons in sections of physically flattened cortex (**A**) and in parasagittal sections of the lateral geniculate nucleus (LGN) (**B**). The cortical labeling is reconstructed from the cumulative charts of six 40 μm thick sections cut in a plane *parallel to the cortical surface* after physically flattening cortex. The black regions labeled FB and DY represent the presumed uptake regions of the dyes. Small dots illustrate DY-labeled neurons, large dots FB-labeled neurons. In the central regions of the zones of labeling, there are many more labeled neurons than there are dots, whereas, in the periphery of the labeled zone, each dot represents a labeled neuron. Broken lines indicate boundaries between areas 17, 18, and 19. Positions of microelectrode penetrations are indicated by numbers. DY, diamidino yellow; FB, fast blue; DL, double-labeled cell.

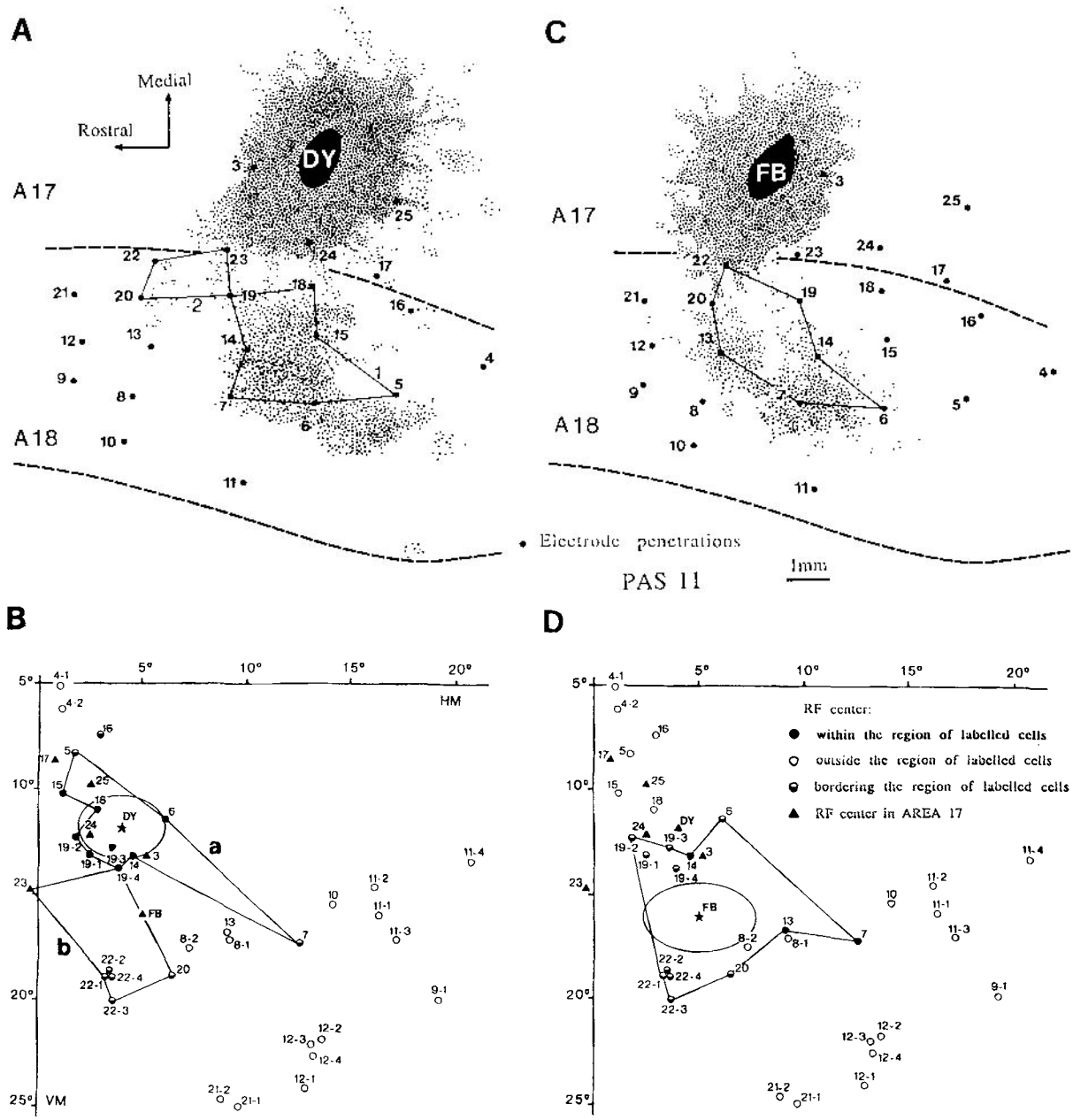

Fig. 3. Visual field representation in the labeled zone for the case illustrated in Figure 2. Upper part of this figure (A and C) shows the distributions of labeled neurons after the DY (**A**) and FB (**C**) injections. Numbers refer to electrode penetrations in the electrode mapping study. Lower part of the figure shows the positions of the receptive field (RF) centers of neurons recorded in areas 17 and 18. Small full circles in **B** and **D** correspond to RF centers of neurons recorded within the labeled zone; half-filled small circles correspond to RF centers of neurons recorded at the limit of the labeled zone. Open small circles, RF centers of neurons outside of the labeled zone; triangles, RF centers of neurons recorded in area 17; large ellipses labeled DY and FB in B and D, visual field representations of the uptake zones (see text for calculation). To facilitate estimation of the extent of the visual field represented in the labeled zone, a line has been drawn interconnecting the RFs recorded near the periphery of the labeled zone. This gives one or two polygons that have been traced out on the cortical surface. The corresponding regions in visual field are illustrated by the polygons below. VM, vertical meridian; HM, horizontal meridian.

diameter. The columns of labeled cells are mostly spatially separated with a few double-labeled neurons where the two populations intermix. The restricted widths of the columns, their small degree of overlap, and the rare occurence of double-labeled neurons is in accordance with the strict visuotopic organization of the geniculostriate pathway (Tanaka, '83; Salin et al., '89).

The spatial extent of the labeled zones in area 18 is extensive and in all cases showed a number of asymmetries or anisotropies. The tangential cortical sections chosen to compose Figures 2A and 3A and C illustrate the maximum spatial extent of labeling in this experiment. If a line is drawn from the injection site, cutting the area 17/18 border at right angles, it is found that labeled neurons in area 18

stretch further caudally to this line than they do rostrally. The distribution of the labeled zone in area 18 is also more elongated in the rostrocaudal than in the mediolateral direction: in Figure 2A (see also Fig. 3A,C), the main bulk of labeled neurons extends 7–8 mm in the rostrocaudal direction and only 4–4.5 mm in the mediolateral direction. To determine just how representative these values are, we have pooled the results from all animals examined and constructed scattergrams (not shown) of the rostrocaudal and mediolateral extents of the labeled zone in area 18 plotted against the area of the uptake region in area 17. For each scattergram, the convergence (as defined in the introduction) is given by the ordinate of the intersection between the regression line and the Y axis. The values of the convergences thus obtained are 5.3 mm in the caudorostral direction and 2.9 mm in the mediolateral direction. Individual values of convergences also enabled us to calculate a mean anisotropy coefficient of 1.8 (ratio of the convergence in the rostrocaudal direction over the convergence in the mediolateral direction).

The wide spatial distribution of labeled neurons illustrates the high convergence of area 18 projections onto area 17. We have estimated the areal extent of the zones of labeling in area 18 and of the corresponding uptake zones of the injections sites in area 17 (Table 1). Similar values were found for supra- and infragranular layers. The values obtained demonstrate the large mismatch found in all cases between these two regions (Table 1). For example, in PAS11 (Fig. 2), the zone of FB labeling in area 18 occupies a surface of approximately 9 mm^2, which corresponds to 9% of the total surface area of area 18, whereas the uptake zone in area 17 is equal to 0.9 mm^2 (which corresponds to 0.5% of area 17).

Extent of the visual field represented in the labeled zone

In all cases, the visual field representation of the area 18 labeled zone was found to be more extensive than that of its uptake zone in area 17. To quantify this mismatch, we have first compared the regions of visual field covered by the centers of the RFs of neurons contained in the labeled and uptake zones. By taking RF centers, we avoided introducing a bias due to the fact that RFs are bigger in area 18 than in area 17. Figure 3B and D illustrate the positions of the RF centers recorded throughout the labeled zones for the DY and FB injections in PAS11. The RF centers recorded in area 17 are represented by triangles and those in area 18 by small circles. Numbers refer to the positions of the electrode penetrations on the cortical surface, which are shown with respect to the labeled zones in Figure 3A and C.

The extent of visual space containing the RF centers of neurons belonging to the uptake zone is determined in the following way. Once the material has been processed for histology, the dimensions along the elevation and azimuth axes are calculated by the formula: $D = d/M + s$ where d is the dimension of the uptake zone along the rostrocaudal or mediolateral axis, M the magnification factor at this eccentricity (Tusa et al., '78), and s the scatter of RF centers (s is assumed to be equal to the mean RF size at this eccentricity; values taken from Dreher et al., '80). In Figures 3–6, the large oval shapes indicate the extent of visual field as calculated above and provide an estimate of the spread of RF centers of neurons included in the uptake zone.

To facilitate understanding of the representation of visual space in the labeled zone, we have made an outline of the visual space explored that approximately surrounds the zone of labeling in area 18. In Figure 3B and D, RF centers recorded inside the labeled zones in area 18 are indicated by small full circles, those situated at the periphery by half-filled circles, and those recorded outside the labeled zone by empty circles. The polygon that surrounds the zone of labeling is traced out by linking those RF centers nearest the periphery of the labeled zone. For the DY label (Fig. 3A), this leads to two polygons, one (a) connecting receptive fields in penetrations 19, 14, 7, 6, 5, 15, 18, 19, and a second (b) formed by linking centers in penetrations 19, 20, 22, 23, 19. Polygon a in Figure 3A includes the greater part of the labeled zone. The region of visual space included in the corresponding polygon a in Figure 3B contains virtually all of the oval region of visual field represented in the uptake zone in area 17. Polygon b in Figure 3A covers a rostral part of the labeled zone corresponding to a relatively low density of labeled cells (see below). None of the RF centers included in the corresponding polygon b in Figure 3B overlap the representation of the uptake zone.

In the case of the FB injection (Fig. 3C,D) the major part of the zone of labeling in area 18 is included in a single polygon formed by interconnecting RF centers in penetrations 19, 14, 6, 7, 13, 20, 22, 19, as shown in Figure 3C. This polygon encircles the oval region of visual space represented in the uptake zone (Fig. 3D). Inspection of the polygons traced out on the labeled zones for both FB and DY injections shows that our visual field mapping did not include all of the zone of labeling. Nevertheless, these results clearly demonstrate that the region of area 18 containing labeled cells encodes a much larger visual field region than that represented in the uptake zone of the injection site in area 17.

Representation of visual space in relationship to labeled cell density

Injections in area 17 did not lead to an even distribution of labeled neurons in area 18. Instead, backfilled neurons in the labeled zones showed characteristic density fluctuations. Various numbers of peaks of high densities were separated by valleys of variable width and, towards the periphery of the labeled zones, there was generally a rim of low labeling density. It could be therefore that regions of the labeled zone that encode visual space distant from the region encoded in the uptake zone might be composed of a few scattered cells. To address this issue we have analyzed cell density gradients across the zone of labeling and examined how this relates to the representation of the visual field. Figures 4 and 5 provide examples of such an analysis. In this animal (PAS16), two injections were placed side by side and separated by 1 mm, one of rhodamine-labeled microspheres (Rh) and another of DY. The injections sites were located 1.2 mm away from the area 17–18 border, close to the representation of the area centralis. Because of the configuration of cortex in this region, mapping was done by making long penetrations along the medial bank of the lateral sulcus, the positions of recording sites were recorded with several lesions in each track, and a two-dimensional reconstruction of the cortex was made by the method of Van Essen and Maunsell ('80).

In the lower part of Figures 4 and 5 are shown the positions of the RF centers recorded in the mapping experiment. The same conventions as in Figure 3 are used to indicate the RF centers of neurons recorded within, at the limit, or outside the labeled zone. To facilitate decipher-

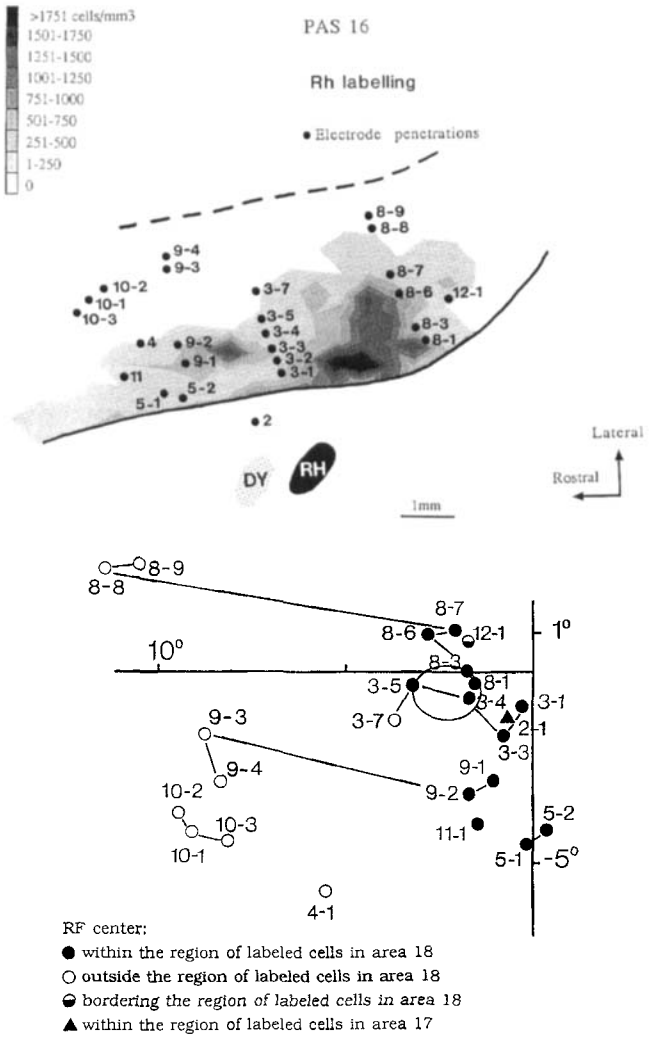

Fig. 4. Labeling density map and visual field map for injections in central visual field representation. **Upper:** Labeled cell density map in area 18 after injection of Rh in area 17 in case PAS16. Cell densities were reported on a 2-D reconstruction made from parasagittal sections by using the method of Van Essen and Maunsell ('80). Numbered dots on the density map refer to recording sites in penetrations running down the lateral gyrus. **Lower:** RF center positions of neurons recorded in the penetrations illustrated above. RFs recorded within the same penetration are linked together. Rh, rhodamine-labeled latex microspheres. Black oval region labeled Rh illustrates the uptake zone for the Rh injection. Ellipse in lower part of figure represents the region containing RF centers of neurons in the uptake zone. Other conventions as in Figures 2 and 3.

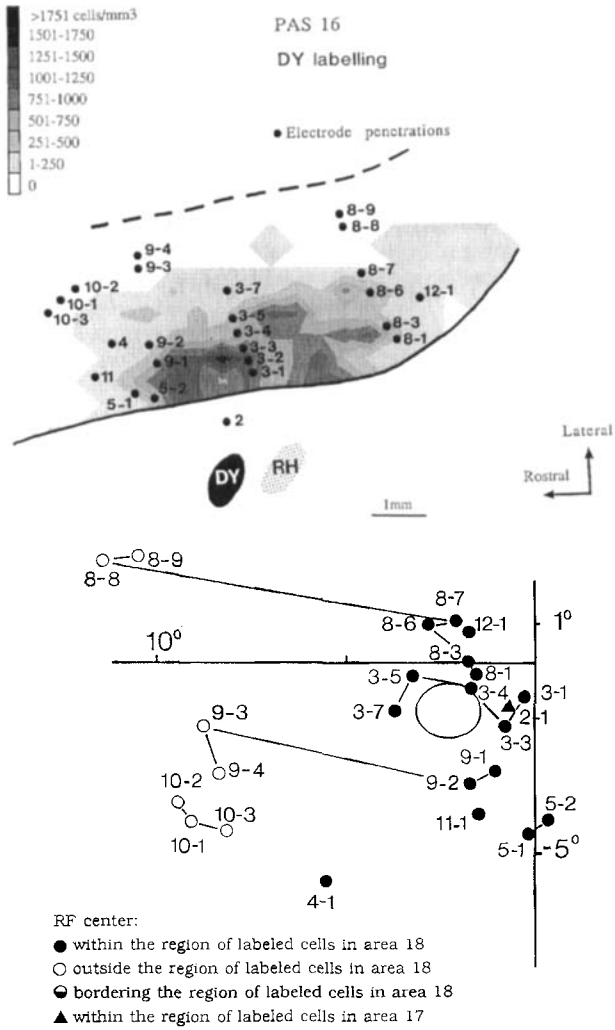

Fig. 5. Labeled cell density map and visual field map of the labeled zone in area 18, following injection of DY in a region of area 17 representing central visual field. Black oval region labeled DY, DY uptake zone. Same animal, data presentation, and conventions as in Figure 4.

ing the representation of visual space in the labeled region, the centers of the RFs recorded every 0.5–1 mm within each penetration have been interconnected. In none of the illustrated cases was a penetration placed exactly in the region of the highest peak of labeled cell density. Nevertheless, it is likely that this region encodes a visual field region situated within the representation of the uptake zone since, in the case illustrated in Figure 4, penetrations 3 and 8, which straddle the highest density peak, returned RFs that also straddle the representation of the uptake zone. A similar observation holds for penetrations 3 and 9 in Figure 5. Further, Figure 5 demonstrates that some secondary density peaks may have visual field representations located outside of the representation of the uptake zone. An example is provided by the peak located near recording point 8.6 in Figure 5.

Although the peak of labeling density most likely encodes a region of visual field situated within the uptake zone representation, regions of area 18 with low labeled cell density also have representations which coincide with that of the uptake zone. This is well illustrated in penetration 3 in Figure 4. Despite the fact that some RFs recorded in this penetration are contained in the representation of the uptake zone (3.4, 3.5), the densities of labeled cells surrounding this penetration are low, as illustrated by the recording points 3.4 and 3.5.

To test more precisely the relationship between labeled cell density and position in visual field with respect to the representation of the uptake zone, in one case (PAS28), we have reconstructed the map of labeling density with a finer grain (200 μm instead of 400 μm). The results of this

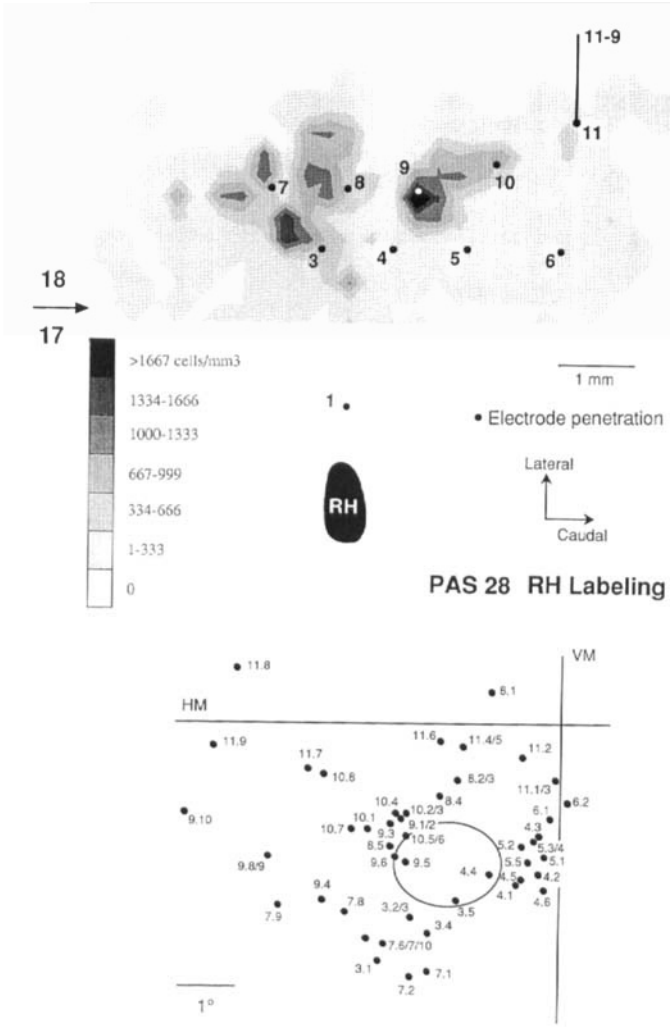

Fig. 6. Density map of cells labeled by rhodamine-labeled latex microspheres (Rh) and positions of RF centers of neurons recorded in the labeled zone in case PAS28 (finer grain map than cases illustrated in Figs. 4, 5). **Upper:** Density map made on cortical surface reconstructed from coronal sections. Rh uptake zone represented in black (injection site shown in coronal section in Fig. 12). **Lower:** RF centers of neurons recorded in the penetrations illustrated on the density map above. Elliptical region corresponds to the representation of the uptake zone (see text). Note that penetration 9, which is located at the peak of labeling density, gave RF centers contained in the representation of the uptake zone. VM, vertical meridian; HM, horizontal meridian.

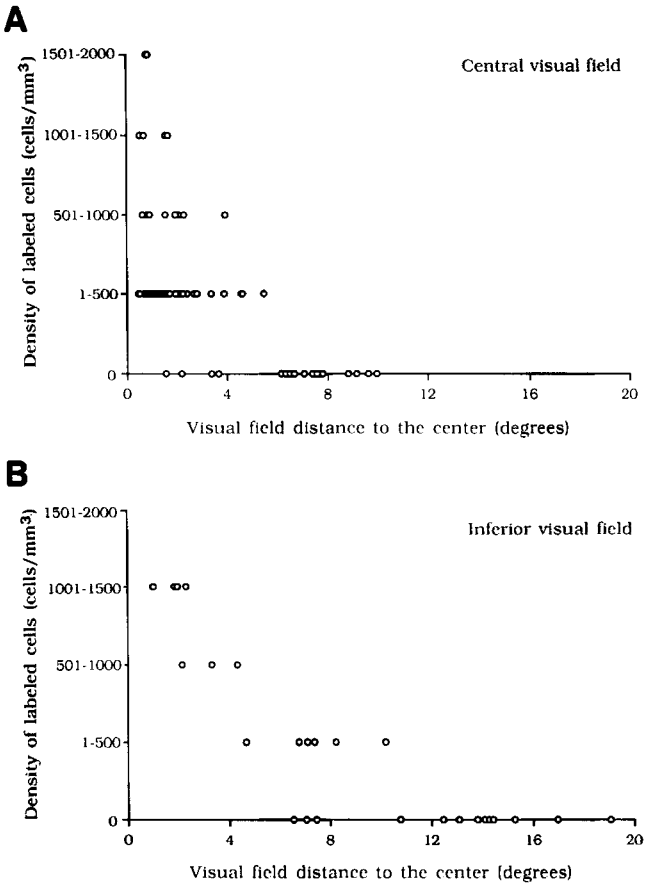

Fig. 7. Scattergrams of the density of labeled cells versus the distance between the RF centers and the center of the visual field representation of the uptake zone for neurons recorded in penetrations in cases PAS16 and PAS28 (**A**) and PAS11 (**B**). Injections in PAS16 and PAS28 were made in regions of cortex representing central visual field (A); injection in PAS11 was made in cortex subserving lower visual field (B).

experiment are presented in Figure 6, in which the map of labeling density was reconstructed from coronal sections and represents the average density throughout the cortical thickness. The most obvious characteristic of Figure 6 compared to Figures 4 and 5 is the more pronounced patchiness of the labeling. This is likely to result mainly from the finer grain of the density map.

The relationship between labeled cell density and position of RF centers with respect to the representation of the uptake zone noted in Figures 4 and 5 is also found in this high-resolution map (Fig. 6). Penetration 9 is situated right at the highest peak of labeling density, and many of the corresponding RFs are located within the uptake zone representation. The last three recording sites (9.8–9.10) have RF centers clearly outside the representation of the uptake zone, possibly because they were recorded outside the region of peak labeling since the penetration was not perfectly normal to the cortical surface. The other important point concerns penetrations 4 and 5. Despite the fact that RF centers are at similar positions with respect to the uptake zone representation as RFs recorded in penetration 9, the labeling density is low in the regions surrounding penetrations 4 and 5. These two observations again underscore that the highest peak of labeling corresponds to the representation of the uptake zone but that not all regions of area 18 in retinotopic correspondence with the uptake zone contain high densities of labeled cells.

Figure 6 also illustrates the presence of minor labeling density peaks. The closest peak to penetration 7 is likely to represent visual field outside the representation of the uptake zone, as suggested by the positions of the RFs of cells recorded in that penetration. The same conclusion also holds for the two peaks located rostral to penetration 7 since, due to the retinotopic organization of area 18, their visual field representation is likely to be located further

away from the representation of the uptake zone than is that of penetration 7.

The relationship between labeled cell density and visual field position is summarized in the scattergrams of Figure 7 concerning the results obtained in cases PAS16 and PAS28 for injections in cortex subserving central vision (Fig. 7A) and PAS11 corresponding to an injection placed in cortex representing peripheral visual field (Fig. 7B). The abscissa indicates the mismatch between RF positions recorded in the labeled zone and the visual field representation at the uptake zone. This is done by measuring the distance between the average RF center of neurons recorded within a penetration in the labeled zone and the center of the representation of the visual field in the uptake zone. Figure 7 demonstrates that in all cases examined, the highest labeling densities are associated with visuotopic correspondence between labeled and uptake zones (distances less than 2° in central visual field and 4° in peripheral visual field). Note that an absence of labeling (i.e., zero on the ordinate) can also be found in regions of area 18 in visuotopic correspondence with the uptake zone (Fig. 7A). Labeled cells are found with RF centers up to 6° distant from the center of the uptake zone representation for central visual field (Fig. 7A) and 10° for peripheral visual field (Fig. 7B).

Quantitative analysis of the labeled region and its visual field representation

Within the sample of cases presented, several corresponded to injections in the cortex subserving the representation of the lower visual field (PAS8, 11, 14) and others to injections close to the representation of the area centralis (PAS16, 28). It is therefore possible to determine the effect of eccentricity on the shape and size of the labeled region and its visual field representation. Cases of injections in cortex subserving the peripheral visual field are presented in Figure 3 and cases of central injections in Figures 4–6. Comparison of these figures demonstrates that the same general features are apparent in both: the labeled region is anisotropic and contains a number of labeling density peaks scattered over a background region of lower density. The ranges of density values are also similar.

One important result stemming from the comparison of peripheral and central cases is the invariance in the size of the labeled zone. This is illustrated in Figure 8A, which presents the area of the labeled zone in area 18 as a function of the eccentricity of the injection site in area 17 for all the cases examined (see also Table 1). Central and peripheral injections returned similar values for the area of the labeled zone (mean 11.4 mm^2 for peripheral and 10.7 mm^2 for central injections).

Given the invariance of the size of the labeled zone with eccentricity coupled with the large variation of magnification factor and RF size with eccentricity, one would predict that the visual field represented in the labeled zone differs for injections in cortex representing central and peripheral visual field. In order to test this, we have estimated the extent of visual field encoded in the labeled zone in area 18 and in the uptake zone in area 17 by the aggregate RF (Dow et al., '81), which reflects both RF size and scatter of RFs and not just the scatter of RF centers as in Figures 3–6. The aggregate RF of the labeled zone is obtained by measuring the total area of visual space occupied by the collection of the smallest RFs encountered in each of the penetrations within the zone of labeling in area 18 (gray region in Fig.

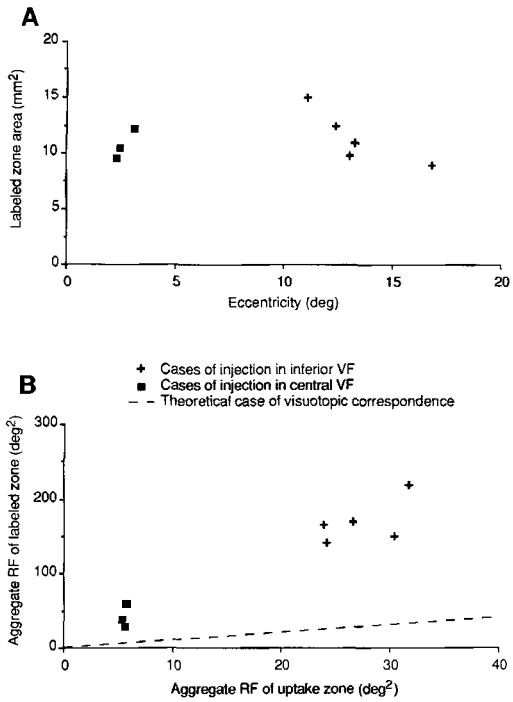

Fig. 8. **A:** Scattergram showing the area of the labelled zone against the eccentricity of the visual field (VF) representation of the injection site. Crosses represent injections in the representation of peripheral visual field, whereas squares represent data concerning injections in the representation of the central visual field. This scattergram shows that the area of the labeled zone does not depend on the eccentricity of the representation of the injection site. **B:** scattergram of the area of the aggregate receptive field (RF) of the labeled zone against that of the uptake zone aggregate RF. The dotted line shows the theoretical case of connections between areas 18 and 17 linking visuotopically corresponding regions. This figure shows that there is a large mismatch in the extent of visual field represented in the uptake and labeled zones and that this mismatch increases with eccentricity.

10). We have also computed the dimensions of the aggregate RF of the uptake zone along the elevation and azimuth by adding the mean RF size to the values computed for the dimensions of the region containing the RF centers (see above) and calculated the area of the corresponding ellipse in visual degrees. The area of the aggregate RF of the labeled and uptake zones for the different cases is presented in Table 1 and as a scattergram in Figure 8B. The dashed line represents the expected relationship between the aggregate RFs of the uptake and labeled zones in case of perfect visuotopic correspondence between both regions (both coding the same extent of visual field). Clearly, the extent of visual field represented in the labeled region is much larger than that in the uptake region. Despite the invariance of the size of the labeled region in area 18 with eccentricity, there is a larger departure from the dashed line in the cases of injections in cortex representing peripheral visual field, reflecting larger RF sizes and scatter in this region.

We have attempted to deduce from the data the extent of visual field represented in the region of area 18 projecting to an infinitely small injection site, coresponding to a virtual point in area 17. Because of sample size, this analysis was carried out only for the injections in cortex subserving peripheral visual field. We made a scattergram of the area of the aggregate RF of the labeled zone as a function of the

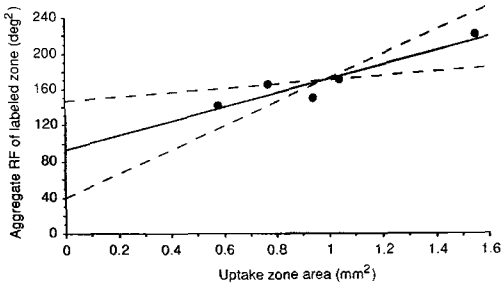

Fig. 9. Scattergram of the area of aggregate receptive field (RF) of the labeled zone in area 18 versus the area of the uptake zone in area 17. The regression line (central line correl. coeff. 0.93) allows the estimation of the aggregate RF area of the convergence region (dotted lines are 95% confidence interval).

area of the uptake zone (Fig. 9) and we fitted the data with a regression line. The intercept with the Y axis corresponds to the predicted value of the aggregate RF of the region of area 18 containing neurons projecting to a virtual point in area 17 (region defined as the convergence region). This predicted value is 94 deg² (40–146 deg², 95% conf. interval) corresponding to a circular region 11° in diameter, for the aggregate RF of an infinitely small injection site. This value is much larger than the aggregate RF of a virtual point in area 17 (4° diameter circle at that eccentricity).

Visuotopic organization of the extrinsic labeled zone

So far our results show that the projections from area 18 to area 17 do not conform to a strict visuotopic organization since neurons were recorded in the labeled zone that had RF centers situated outside the region of visual space containing the RF centers in the uptake zone. To estimate the extent of this departure from strict visuotopy it is necessary to have an estimation of the degree of mismatch taking into account the sizes of the RFs. This is done using aggregate RFs as a measure of the visual field coded in the labeled and uptake zones (see above). Typical results of this analysis are shown in Figure 10 for the FB injection in PAS11. On the left-hand side are shown in gray the smallest RFs from each penetration made in the labeled zone, together with the aggregate RF of the uptake zone (indicated by an ellipse and computed as above; note that the ellipse in Fig. 10 is larger than that in Fig. 3, which did not take into account the RF size). This figure shows that, despite its anisotropy, the labeled zone represents a broadly isotropic region in visual field and that the RFs of cells within this region are in close proximity to the aggregate RF of the uptake zone.

On the right-hand side of the lower half of the figure are shown the RFs of cells recorded outside the labeled zone. They are situated at some distance from the aggregate RF of the uptake zone except for the RFs recorded in penetration 8. In this penetration RFs were very large, often including the whole contralateral hemifield. This region of cortex most likely corresponds to the islands of area 18 containing the peripheral representation (Donaldson and Whitteridge, '77; Albus and Beckmann, '80) and our results suggest that the neurons of these regions do not necessarily have more widespread extrinsic connections to area 17.

The isotropy of the aggregate RF of the labeled region was found in all cases examined, independently of whether

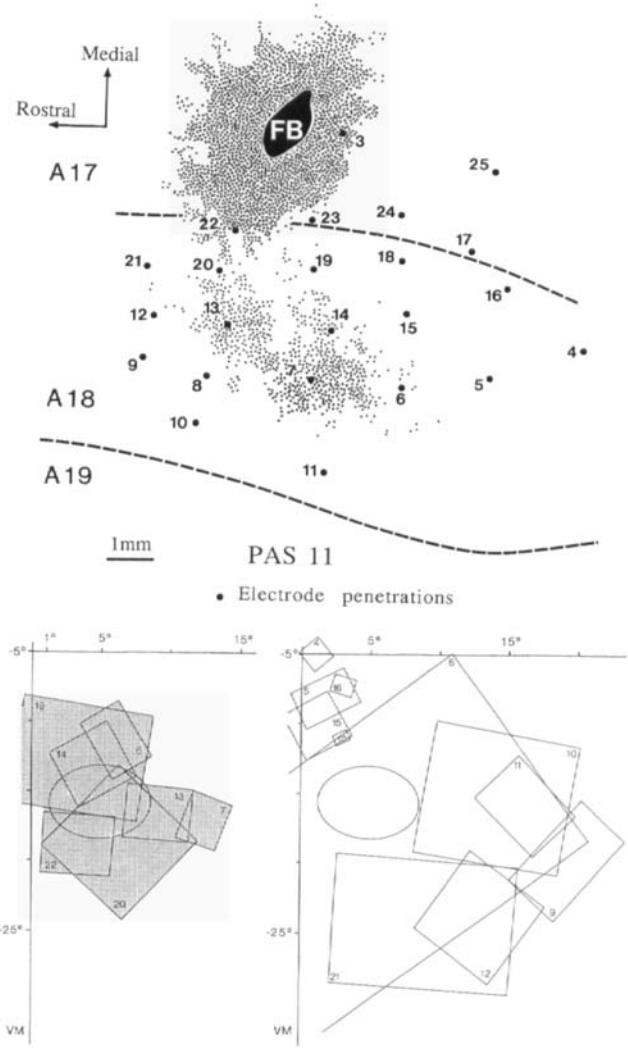

Fig. 10. Aggregate RF of the labeled zone. Same case illustrated in Figures 2 and 3. On the left are shown the smallest RFs recorded in each of the penetrations situated within the labeled zone. The resulting gray region is called the aggregate RF of the labeled zone. On the right are shown the RF plots recorded from area 18 neurons located outside the labeled zone. In this figure, the ellipse represents the aggregate RF of the uptake zone (larger than the uptake zone representation illustrated by the ellipse in Fig. 3D; see text). FB, fast blue; VM, vertical meridian.

the injection was in cortex subserving central or peripheral visual field.

We then attempted to determine whether interconected regions in areas 17 and 18 contain neurons with overlapping receptive fields. We used several approaches to answer this question. One was to sample the periphery of the region of labeling in area 18. The results of this experiment are presented in Figure 11. The analysis was restricted to the supragranular layers in which many neurons projecting to area 17 are found (Bullier et al., '84a; Symonds and Rosenquist, '84). The results illustrated in Figure 11 show that RFs recorded at the perimeter of the labeled zone had centers located 5–10° from the aggregate RF of the uptake zone and only a few showed some degree of overlap with that region.

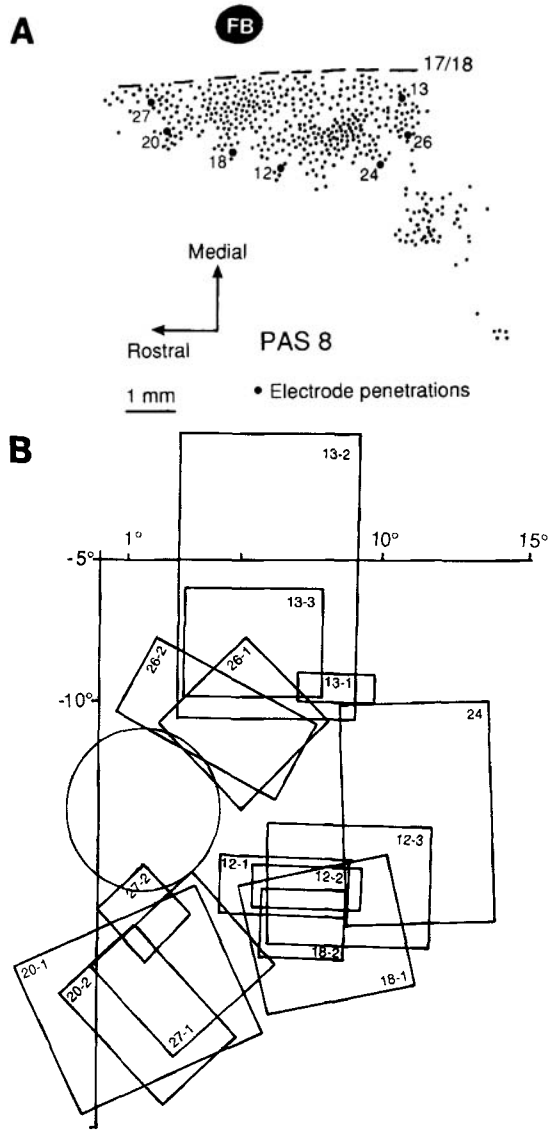

Fig. 11. Lack of overlap (nonvisuotopy) between the RFs of neurons recorded in the periphery of the labeled zone and the aggregate RF of the uptake zone. **A:** Distribution of fast blue (FB)-labeled neurons in supragranular layers from one section cut parallel to the cortical surface of flattened cortex. **B:** RF plots of neurons recorded in penetrations illustrated above. Ellipse indicates the aggregate RF of the uptake zone. This figure suggests that nonvisuotopic connections exist between supragranular layer neurons in area 18 and neurons in the uptake zone in area 17.

So far we have examined the visual representation of the labeled zone by recording a few neurons per penetration, mostly in the supragranular layers so as to be able to maximize the number of penetrations in the limited time available and to obtain a complete visuotopic map of the zone of labeling. However, given the large degree of RF scatter in area 18, it could be objected that if we had recorded more RFs per penetration we would have found *a larger* degree of RF overlap with the aggregate RF of the uptake zone, when one or two fields per penetration showed apparent separation. We have therefore undertaken mapping studies in which multiunit activity was recorded every 100–200 μm in fewer penetrations aimed at the labeled zone. Reconstructions of the penetrations were made with the help of the lesions placed during the experiment (all penetrations shown in Figs. 12 and 13 contained several lesions). Figure 12 presents the results of such a mapping experiment taken from the same case illustrated in Figure 7. Three penetrations are illustrated on coronal sections. Penetration 1 was placed in the middle of the injection site in area 17. The corresponding RFs are contained within the oval region corresponding to the aggregate RF of the uptake zone. Two penetrations in the labeled region in area 18 are also illustrated. Penetration 7 is located next to one of the minor peaks of labeling density (see Fig. 7). Although all neurons within this penetration have RF centers that were clearly nonoverlaping with RF centers in the uptake zone (Fig. 7), several RFs showed a slight degree of overlap with the aggregate RF of the uptake zone (Fig. 12). A similar overlap was found for neurons recorded in penetration 11, which is located close to the caudal extremity of the labeled region in a zone of low labeling density (see Fig. 7).

In the same animal we also made an injection of FB and examined the relationship between the labeling and the position of RFs with respect to the aggregate RF of the uptake zone. The results are presented in Figure 13 on three coronal sections. The lower section (number 304) illustrates the injection site with penetration 2 running through the middle of the uptake zone. The RFs recorded in penetration 2 are illustrated within the circular region representing the aggregate RF of the uptake zone. Two penetrations made in the periphery of the labeled zone are illustrated on sections 244 and 253 situated respectively 2.9 mm and 2.45 mm caudal to section 304 (values corrected for shrinkage). The RFs of practically all neurons recorded in these two penetrations show no overlap with the aggregate RF of the uptake zone. In penetration 4 one of the six RFs touched on the outer perimeter of the aggregate RF of the uptake zone. Likewise in penetration 9, of the ten RFs recorded, only two encroached on the circumference of the aggregate RF of the uptake zone.

The penetrations illustrated on Figures 12 and 13 are representative of the results obtained in these mapping studies: in some penetrations, situated either near the center or in the periphery of the labeled zone, RFs overlapped with the aggregate RF of the uptake region, whereas in other penetrations, most RFs were located outside of it. In every one of the penetrations made in these fine-grain mapping studies, at least one or two RFs showed some contact with the perimeter of the aggregate RF of the uptake zone.

Visuotopic representation of the zone of intrinsic labeling in area 17

In the present study we have two cases that illustrate the extent of the visual field representation in the intrinsic labeled zone in area 17. In the DY injection in PAS11 (Fig. 3) we found three penetrations (3, 17, 25) near the periphery of the intrinsic zone of labeling. Although we did not obtain enough recording points to calculate the aggregate RF, there was clearly a mismatch between the representation of the intrinsic labeled zone and that of the uptake zone since RFs in penetration 3 had centers located 3.7° from the center of the ellipse in Figure 3.

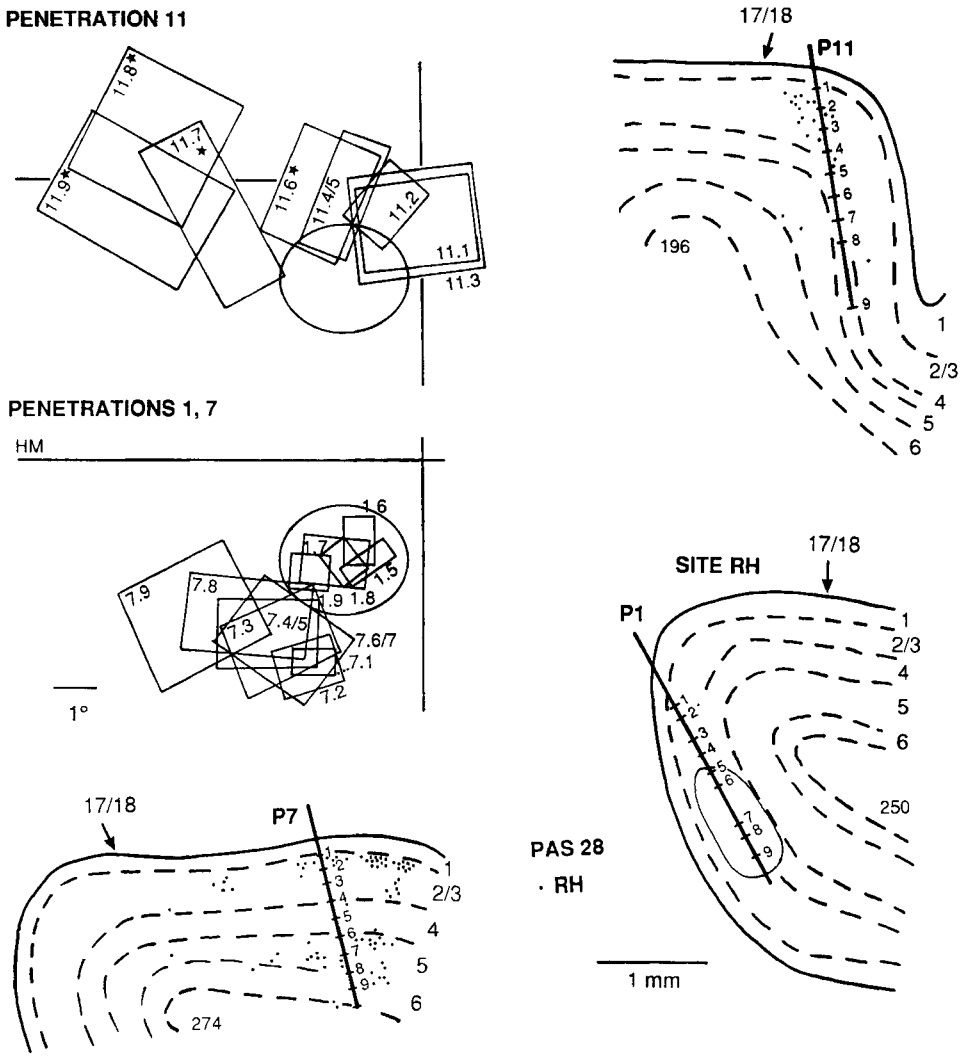

Fig. 12. Examples of penetrations with RFs partially overlapping the uptake zone aggregate RF (ellipse). Case PAS28 Rh (also illustrated in Fig. 7). Penetration 1 is in the injection site in area 17. Penetrations 7 and 11 are in regions of low to medium labeled cell density (Fig. 7). RF plots with asterisks in penetration 11 correspond to recording sites outside the region of labeling. RH, rhodamine-labelled cells; HM, horizontal meridian.

In PAS14, several penetrations were placed within the intrinsic labeled zone, in addition to penetrations mapping the extrinsic labeled zone of the area 18 to 17 connection. This enabled us to compare the aggregate RFs of these two labeled zones. The results are presented in Figure 14. The RFs recorded within the extrinsic labeled zone in area 18 are presented in Figure 14C and the RFs recorded in the intrinsic labeled zone in area 17 in Figure 14B. Although the mapping of the intrinsic labeled zone is incomplete, most penetrations were placed at its caudal and rostral limits. The positions of the corresponding RFs match remarkably well the limits in elevation of the aggregate RF of the labeled zone in area 18. In addition to documenting a clear mismatch in the aggregate RFs of the uptake and labeled zones of the intrinsic connections, this figure makes the important point that the labeled zone of the area 18 to 17 projection encodes a similar extent of visual field as that represented in the intrinsic connections within area 17.

DISCUSSION

The main result of the present study is that connections between areas 17 and 18 are not restricted to linking regions in which RFs are located in the same part of the visual field. Instead, we have found that, although the strongest links are between visuotopically corresponding regions, sparse connections can be found between regions of areas 17 and 18 that do not include a common part of the visual field. Before considering the functional significance of these findings we shall first examine critically the methodology used.

Methodological considerations

A major concern in the present study was to use retrograde tracers that, when injected in cortex, are captured in a volume of cortex that can be precisely determined,

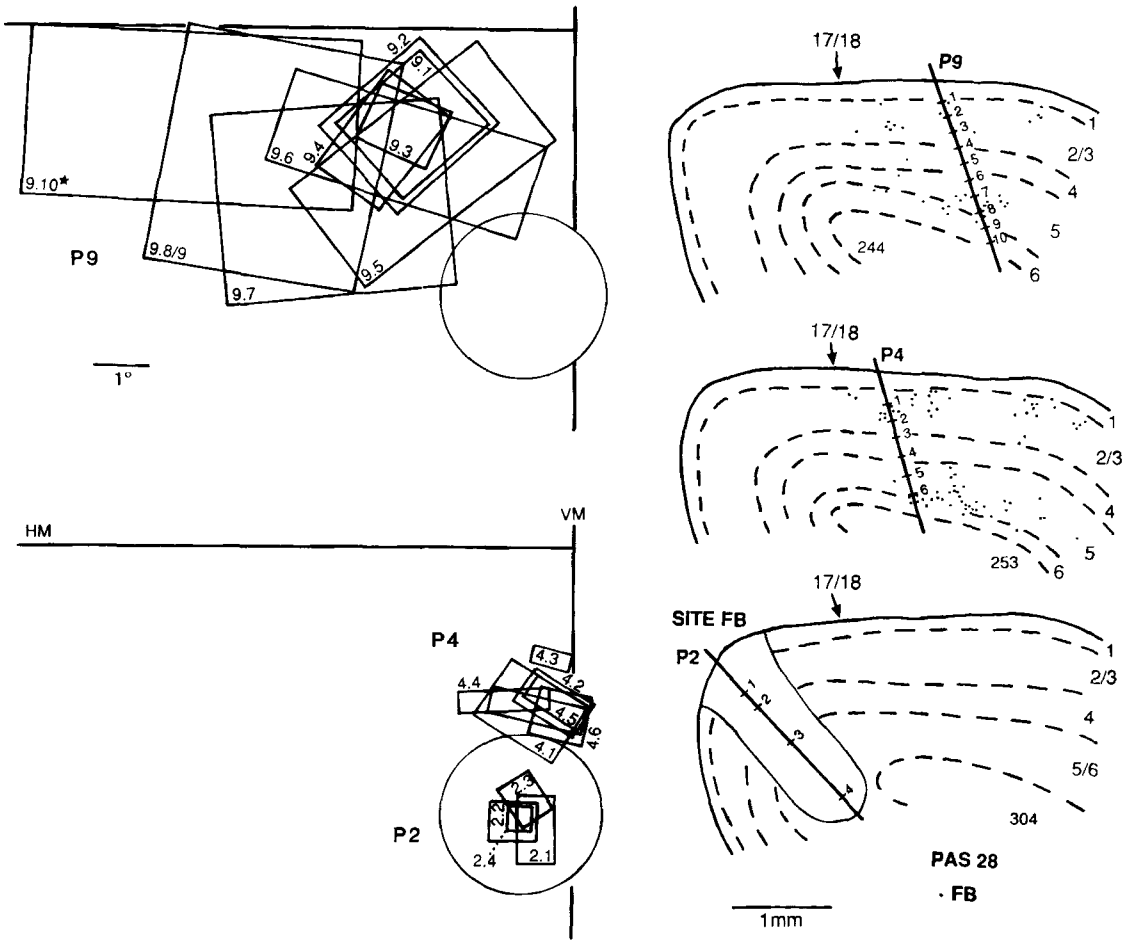

Fig. 13. Examples of penetrations with RFs mostly nonoverlapping the aggregate RF of the uptake zone (circle). Penetration 2 is in the injection site in area 17. Penetrations 4 and 9 are situated at the periphery of the labeled zone. Same conventions as in Figure 12. FB, fast blue; VM, vertical meridian.

thereby giving an uptake zone of known dimensions. Fluorescent dyes and latex microspheres fulfill these criteria and have the added advantage that several distinguishable tracers can be used simultaneously, thereby optimizing the chances of adequate sampling of the labeled zone. The similarity of the results obtained with rhodamine-labeled latex microspheres and fluorescent dyes suggests that our estimation of the uptake regions of the latter are valid. The slow axonal transport of these tracers means, however, that the animals have to recover from curarization for a prolonged survival period. This restricts the duration of the electrode recordings that can be made at the time of injection so that, for several animals, estimation of the extent of the visual field in the uptake zone has been calculated from the average RF size and position from the recording made prior to injection, in conjunction with published magnification values at the eccentricity of this site. This is an important aspect of our study since the mismatch of the visual field representation in the uptake and labeled zones could originate simply from an underestimation of the representation of visual space in the uptake zone. For this reason, we have made extensive mapping of the uptake zones in one case (PAS28). The good fit between the region covered by the RFs of neurons recorded in the uptake zones and the calculated corresponding aggregate RFs (Figs. 12, 13) justifies our use of the estimation of the aggregate RF of the uptake zone in the other cases.

One could argue that mapping the injection site and the labeled regions during different experimental sessions may lead to inaccuracies in the match between the visual field regions represented in the two zones. Two-session mapping was not the general case, however, since in the cases PAS16 and PAS28, for which the mapping of the labeling and the visual field was done with a fine grain, mapping of the uptake zone and labeled regions were done during the same experimental session.

It is known that some connections between adjacent regions of areas 17 and 18 travel in the cortical gray matter (Fisken et al., '75). Capture of the dyes by such fibers of passage would lead to an overestimation of the extent of the labeled zone. This poses a problem for the cases illustrated in Figures 11 and 13 since the uptake regions are located close to the 17–18 border, in a region where the 17–18 connections circulate in gray matter (Henry et al., '91). Uptake by fibers of passage in these cases appears to introduce only minimal distortion, however, since similar results were obtained when the injection was located far from the 17–18 border (e.g., Figs. 6, 12).

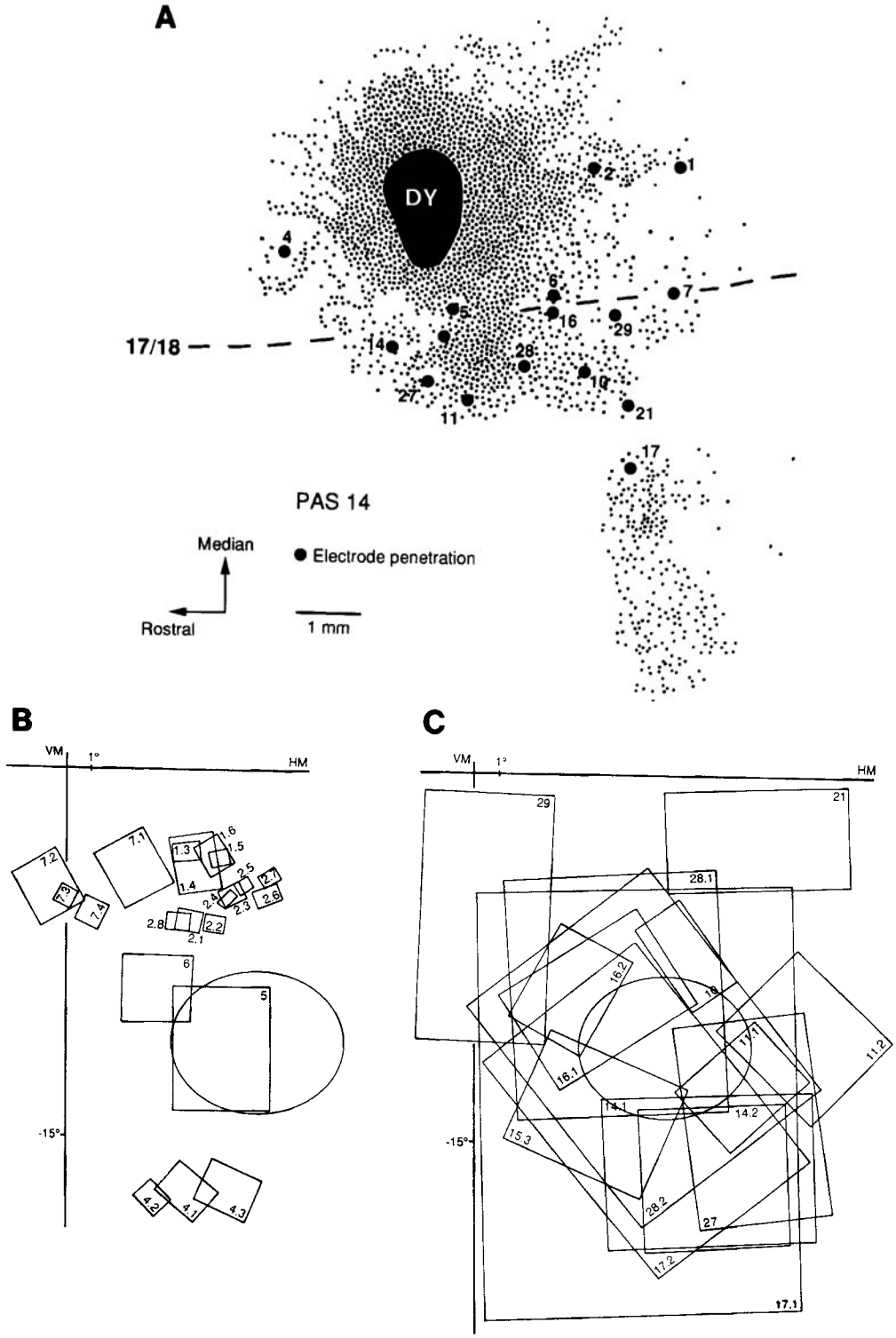

Fig. 14. Comparison between the aggregate RF of the labeled zones in areas 17 and 18. **A:** Distribution of labeled cells in one section in the supragranular layers of the flattened cortex. **B:** RFs of neurons recorded in penetrations within the labeled zone in area 17. **C:** RFs of neurons recorded in penetrations in the labeled zone within area 18. Ellipse represents the aggregate RF of the uptake zone. DY, diamidino-yellow; VM, vertical meridian; HM, horizontal meridian.

A major potential source of error is in the reconstruction of the electrode penetrations in the labeled zone. We have limited it by using stereotaxic coordinates, placing electrolytic lesions every other penetration, and using the penetrations with lesions to extrapolate the positions of the penetrations with no lesions. Since penetrations were separated by

0.5 to 1 mm, the potential error introduced by this procedure does not exceed a few hundred microns, a distance smaller than the grain of our sampling of the labeling density in most cases.

Another methodological limitation is related to the fact that we estimated the extents of individual RFs using a qualitative method, given that quantitative methods, by the use of averaging, reveal regions of the RF that are often subthreshold to qualitative assessment (Orban, '84). For example, the RF width of a complex cell measured with quantitative techniques appears to be larger by a factor of 2 than the qualitative RF size (Kato et al., '78). This does not affect our conclusion of the mismatch between labeled and uptake zone representations since evidence for this is largely based on the positions of RF centers (Figs. 3–6), which show little or no variation in position when measured with quantitative or qualitative methods (Cynader et al., '87). Our conclusion that some RFs recorded at the periphery of the labeled zone do not overlap with the aggregate RF of the uptake zone is more likely to depend on the method used to plot receptive fields. In case PAS28, RF plots were derived from low-threshold multiunit recordings, a method that gives much larger RFs than single-unit recordings, as can be seen when the sizes of RFs recorded with both methods in our own sample are compared. Even in this case, in which there is an overestimation of RF size, we found several examples of penetrations in which few sites had RFs overlaping the aggregate RF of the uptake zone.

Spatial configuration of the labeled zone in area 18

The present results confirm the high degree of convergence of the projections from area 18 to area 17 in the caudorostral direction that we demonstrated previously (Salin et al., '89). In the former study we used relatively large injections of DY and FB (1–3 mm in diameter) and the convergence values were deduced from a geometrical construction. In the present study, using small injections and including a tracer that is known to have a restricted uptake region (Rh, Katz et al., '84; Gilbert and Wiesel, '89; Cornwall and Philippson, '88), we obtain a rostrocaudal convergence value of 5.3 mm. This value is within the range previously reported (3.6–5.8 mm).

The convergence value in the rostrocaudal direction is larger than that in the mediolateral direction. This anisotropy is probably linked to the overall anisotropy of the retinotopic representation in area 18, as reported by Tusa and coworkers ('79). The fact that area 18 is more extended in the rostrocaudal axis may be related to the larger magnification factor in this direction than in the mediolateral axis (Tusa et al., '79; Albus and Beckmann, '80; Cynader et al., '87). Our recordings in the labeled zone in area 18 show it to have a broadly isotropic representation of the visual field. The pronounced anatomical anisotropy that we have observed in the labeled zone in area 18 may simply arise from the necessity to compensate for the anisotropic magnification factor in area 18 so as to maintain a broadly isotropic aggregate RF for the labeled zone.

There are striking similarities in the spatial configuration of the labeled zone in area 18, as shown in the present study, and the distribution of intrinsic neurons projecting to a point within area 18 as reported in the studies of Matsubara et al. ('87) and Levay ('88). These similarities include anisotropy coefficient (1.8 in the present study and 2 in the study of Matsubara et al., '87) as well as the fact that labeled neurons in both intrinsic and extrinsic labeled zones within area 18 stretch further in the caudal direction (i.e., towards the representation of the area centralis) than they do rostrally (i.e., towards the peripheral representation).

At present, we can only speculate on the similarity of the organizations of intrinsic and extrinsic labeling in area 18. For instance, in the intrinsic labeled zone, labeled neurons are distributed in patches (Matsubara et al., '87; Price, '86; LeVay, '88; Gilbert and Wiesel, '89). In the present study, we have also found evidence of fluctuations of cell density across the extrinsic labeled zone, which, although less pronounced than in the reciprocal pathway (Gilbert and Kelly, '75; Symonds and Rosenquist, '84; Bullier et al., '84b; Ferrer et al., '88; Gilbert and Wiesel, '89), are nevertheless observed in all cases. It is conceivable that the patches in both intrinsic and extrinsic labeled zones in area 18 would coincide if injections were placed in regions of areas 17 and 18 sharing the same visuotopic and orientation specificity (see below). If this were so, both of these cortical pathways could be provided by the same neurons sending one axon to area 17 and another locally to area 18. This possibility is in accordance with the fact that all pyramidal cells that have been shown to have an extrinsic projecting axon also possess a long-range intrinsic projection (Douglas and Martin, '90).

The present results also demonstrate that injections in area 17 lead to similar sizes of labeled zones in area 18 irrespective of whether they concern cortex subserving the central or peripheral visual field. This constancy is all the more significant in view of the large differences in magnification factor between these two regions of area 18 and suggests that the size of the convergence zone is dictated by morphological parameters such as the dimensions of extrinsic axonal arbors. The constancy of convergence is yet another feature that underscores the often described crystal-like organization of the cortex (Hubel and Wiesel, '74; Albus, '75; Jones et al., '75).

Visuotopic correspondence between interconnected regions in the cortex

The finding in the present report that the extent of the visual field representation is greater in the labeled zone in area 18 than in the uptake zone in area 17 needs to be considered in light of what is known about other cortical pathways. Earlier reports, mostly based on anatomical results (Gilbert and Wiesel, '83; Martin and Whitteridge, '84; Kisvarday et al., '86; Luhmann et al., '90) and the results presented in Figure 14 suggest a similar visuotopic mismatch for intrinsic connections within area 17. Consideration of the extent of cortex occupied by labeled neurons in area 18 after injections in that area (Matsubara et al., '87; LeVay, '88) leads to a similar conclusion concerning the intrinsic connections within area 18. Further, there is overwhelming evidence that the connections linking the cerebral hemispheres also interconnect nonvisuotopically corresponding zones (reviewed in Kennedy et al., '91).

Cortical pathways have been described that link together visuotopically corresponding regions. This has been reported for the projections from area 17 to area 18 (Ferrer et al., '88; Salin, '88) and for the projection from area 17 to the Clare-Bishop area (Sherk and Ombrellaro, '88). It would be

interesting to determine whether this is a general feature of all output projections from area 17.

Whether or not the aggregate RF of the labeled zone matches with that of the uptake zone does not depend on the convergence value being large or small. For example, the projection from area 17 to area 18, for which there is a match, has a similar convergence value (5.45 mm, Salin et al., unpublished results; Gilbert and Wiesel, '89) as the reciprocal pathway (5.3 mm; present study), which presents a mismatch. The retinotopic organizations of the source and target areas, on the other hand, constitute important parameters for the question of visuotopic correspondence. It is well established that area 17 has smaller RF sizes and RF scatter than neurons in other cortical areas (Hubel and Wiesel, '63, '65; Albus, '75; Spear and Baumann, '75; Palmer et al., '78; Dreher et al., '80; Tusa and Palmer, '80; Ferster, '81; Duysens et al., '82; Cyander et al., '87). Even if we assume that all cortical areas that project to area 17 had a point-to-point connectivity, if RF size and scatter in the source areas were larger than in area 17, this would lead to a greater representation of the visual field in the labeled zone than in its uptake zone in area 17. In other words, even assuming a hypothetical (and as yet unobserved) point-to-point connectivity, there will be a lack of visuotopic correspondence when the source has larger RFs than the target area. One would therefore predict that in other species, such as the monkey, in which there is a similar increase in RF size and scatter as one goes from striate to extrastriate cortex (Allman and Kaas, '74; Gattass et al., '85, '88), the feedback projections from extrastriate to striate cortex will also show a lack of visuotopic correspondence between interconnected regions.

The question of matching visual field representations in interconnected regions is relevant to the current dichotomy between feedforward and feedback connections (Tigges et al., '77; Rockland and Pandya, '79; Wong-Riley, '79b; Van Essen and Maunsell, '83; Kennedy and Bullier, '85). From results in the cat mentioned above (Salin, '88; Ferrer et al., '88; Sherk and Ombrellaro, '88), it appears that feedforward connections may interconnect visuotopically corresponding regions. If this should always be the case, then the presence or absence of visuotopic correspondence between interconnected zones could well constitute, along with laminar location of parent cell bodies and axon terminals, another characteristic difference between feedforward and feedback cortical pathways.

A virtual point in area 17 receives converging input from numerous cortical areas. The question then arises of whether the visual field regions represented in the individual labeled zones match in each of the afferent cortical areas. Our results demonstrate a match between the visual field representation in the labeled zones in areas 18 and 17 (Fig. 14). A similar conclusion can be reached when the visual field encoded in the labeled region in area 17 is estimated from the study of Gilbert and Wiesel ('89) together with the mapping data of Tusa et al. ('78). It is possible to calculate the representation in the labeled zone in area 19 following injection in area 17 and this also appears to follow the same rule. Hence, knowing the convergence value for the projection from area 19 to area 17 (Salin et al., '89) and the retinotopic organization of area 19 (Tusa et al., '79; Albus and Beckman, '80; Dreher et al., '80) we can estimate that the area 19 convergence zone encodes 15–20° in cortex subserving eccentricities of 12° in lower visual field. This value is derived from average sizes and scatter of RFs in area 19. If the smallest RFs in each penetration were used for this calculation, as was the case for areas 17 and 18, the resulting diameter of the aggregate RF of the convergence region would be close to the value of 11° found for the convergences of areas 17 and 18.

These results mean that, for any given population of neurons projecting to a column of neurons in area 17, each encodes the same extent of the visual field, irrespective of whether it is located in areas 17, 18, or 19. Consequently, a column of neurons in area 17 has direct access to information concerning a region of the visual field, which we call the convergence window, which measures 11° in diameter in cortex subserving peripheral visual field and which is encoded in areas 17, 18, and 19.

One may therefore wonder whether callosal connections also obey a similar rule of connectivity. These connections also present large convergence zones (Payne, '90; Kennedy et al., '91). When the extent of the aggregate RF of the convergence zone is calculated from these data, similar values are found as for the convergence window. This finding implies that a neuron with a RF situated next to the vertical meridian would receive converging influence from two convergence windows, one ipsilateral to its RF and another in the controlateral hemifield. This second window may complete the ipsilateral one, in order to maintain a broadly isotropic convergence window. In this way, neurons with RFs located near the vertical meridian would be influenced by an isotropic convergence window in the same manner as those neurons with RFs located away from the vertical meridian.

Regions in area 18 that are in visuotopic correspondence with the uptake zone are often associated with high labeling densities (Figs. 4–7). This suggests the presence of a particularly dense subset of connections linking visuotopically corresponding regions. However, the presence of low as well as high densities of labeling in regions of the labeled zone in correspondence with the uptake zone suggests that position in visual space is not the only functional parameter governing the strength of connections. One possibility is that dense connectivity interconnects neurons with similar orientation selectivity, as has been shown for the reverse projection (Gilbert and Wiesel, '89). This dense subset of specific connections may also correspond to the one activated by electrical stimulation in area 18 (Bullier et al., '88), which was efficient in driving neurons *only* when the stimulating and recording electrodes were placed in visuotopically corresponding regions. It would be interesting to test whether activation of area 17 neurons by electrical stimulation of area 18 is possible only when the RFs of the stimulated and activated neurons have similar orientation specificity.

Assuming that projections from area 19 are organized in a similar fashion, one would predict that a peak of labeled cell density would also be observed in the region of area 19 in visuotopic correspondence with the uptake zone and containing neurons with similar orientation preferences to those contained in the uptake zone and in the interconnected region in area 18. One sees that in this way, a neuron in area 17 may be interconnected with a dense network of neurons situated in other areas and sharing common RF properties. This leads us to view the classic RF of a given neuron in area 17 not solely as the result of local processing within the area but of the processing occurring within the

extended cortical network in which it is embeded. There is a body of evidence that cortical neurons are contacted by many hundreds of neurons and that the response of a single neuron represents the concerted activity of large populations of afferent neurons (Douglas and Martin, '90). In this case one would predict that the sensitivity profile of the RF of a neuron would be the weighted sum of the RF sensitity profiles of the neurons afferent to it. Because of the enormous number of afferents to a single cortical neuron, it is not surprising that the contribution of a single afferent might go undetected in the RF of the target neuron.

Connections arising from regions of the labeled zone that do not visuotopically correspond to the uptake zone also include peaks of high density of labeled cells (Figs. 4–6). It is likely that these peaks correspond to patches of neurons with RF properties similar to those contained in the uptake zone but with partially or nonoverlapping RFs. A recent cross-correlation study between neurons of areas 17 and 18 suggests that orientation selectivity constitutes an important organizing principle of connections between areas 18 and 17 since temporally coupled neurons with separate RFs tend to possess similar optimal orientation selectivity (Nelson et al., '92). In this way, the connections from area 18 to 17 would conform to the same organization principles as the intrinsic connections of area 17 that are known to link together neurons with similar optimal orientations (Ts'o et al., '86; Engel et al., '90).

It would appear, however, that the connections linking regions out of visuotopic correspondence have different functional characteristics from those interconnecting visuotopically matched regions. This is suggested by the results of electrical stimulation demonstrating the impossibility of driving area 17 neurons from area 18 when the site of electrical stimulation and recording were not visuotopically matched (Bullier et al., '88). The results of cross-correlation studies also suggest that these connections are of a different nature since the temporal coupling between area 17 and 18 neurons is less precise when the RF are not overlapping (Nelson et al., '92).

Thus, connections between areas 17 and 18 can be placed in two categories: those that interconnect visuotopically corresponding regions and those that link regions that are not in correspondence or only in partial correspondence. The connections linking visuotopically corresponding regions would exert a suprathreshold excitation on area 17 neurons while the connections between non- or partially visuotopically corresponding regions would provide a modulatory influence on these neurons. This could be a subthreshold excitatory drive that fails to reach the threshold even when many neurons are electrically coactivated. Such subthreshold excitation by afferent connections has been suggested to play an important role in corticocortical and corticothalamic projections (Sherman and Koch, '86; Deschênes and Hu, '90; Douglas and Martin, '90).

It is also possible that connections linking nonvisuotopically corresponding regions contact interneurons that would exert a rapid inhibitory influence on local area 17 neurons. A balance between excitatory and inhibitory influences may constitute the mechanisms underlying the long-range modulatory effects observed outside the classical RF (Hammond and Mackay, '75; Nelson and Frost, '78; Sillito, '79; Orban et al., '87). It is significant that the size of the modulatory zone of RF of neurons in part of area 17 representing central visual field (Nelson and Frost, '78) is similar to that of the aggregate RF of the labeled zone measured in the present study.

Functional rules governing the spatial organization of corticocortical connections

The retinogeniculostriate and corticotectal pathways are believed to be strictly visuotopically organized in that the RFs of target neurons include the RFs of the source neurons (Cleland et al., '71; McIlwain, '73, '77; Tanaka, '83). The corollary of this is that a single neuron in an uptake zone will have an RF that includes the individual RFs of its afferent neurons in the labeled zone. As mentioned above, there is evidence that projections of area 17 to area 18 might also be organized according to such a principle of strict visuotopy. This type of organization was proposed as a rule of connectivity by McIlwain ('73), who stated that "the cells of the striate cortex, which project functionally to a collicular neuron, also 'look' collectively at the same area of visual space as that collicular cell."

Because of the larger RFs in area 18 than area 17, strict visuotopic correspondence is impossible in the connections from area 18 to area 17. Our results demonstrate that many of the RFs we recorded in the labeled zone in area 18 partially overlap with the aggregate RF of the uptake zone. The consequence is that there are numerous partially visuotopic connections from area 18 to area 17. In this way, neurons of area 18 that project to area 17 collectively look at a larger region of visual field than the cells they project to.

The presence of nonvisuotopic connections between neurons in areas 18 and 17 is difficult to prove with the methods used in the present study. If such nonvisuotopic connections exist, they appear to be limited to a subpopulation of cells located at the border of the labeled zone and in supragranular layers. The situation is different, however, for the intrinsic connections within area 17. Knowing the difference in elevation between the RF positions of neurons at the limit of the labeled zone and in the uptake zone (Fig. 14) and the RF size and scatter within area 17 (Albus, '75; Tusa et al., '78), it is easy to demonstrate that numerous neurons in the labeled zone in area 17 have nonvisuotopic connections with their target neurons. Similarly, since the labeled zone is more extensive (Salin et al., '89) and the RF sizes smaller in area 19 (Dreher et al., '80) than in area 18, it is likely that many connections from area 19 to area 17 are also nonvisuotopic.

Thus, corticocortical connections belonging to the 17-18-19 network do not appear to follow the rule of McIlwain. What, then, is the rule governing the spatial organization of corticocortical connections? The key element appears to be the match between the aggregate RFs of the labeled zones in areas 17 and 18. It would appear that corticocortical connections are organized in such a way as to maintain this constancy of a common window of visual field influencing neurons in area 17. This concept of a common convergence window can be extended to the single cell level. In this way, neurons within area 17, area 18, area 19, and the contralateral cortex would connect to a given neuron in area 17 only if their RF belongs to the convergence window of this neuron, irrespective of whether there is overlap between their RFs.

With this connectivity rule, overlapping RF would no longer be a necessary condition for the presence of interconnections between cortical neurons, and whether individual cell-to-cell connections are visuotopic or not would depend

on the respective sizes and positions of the minimal RFs of the interconnected neurons.

ACKNOWLEDGMENTS

We thank Sandrine Beaumont, Noëlle Boyer, Ghislaine Clain, and Pascale Giroud for technical support. We are grateful to Lea Krubitzer for help with the cortex flattening method. Financial support to P.A. Salin from Bourse Fouassier, Fondation de la Recherche Médicale and Fédération des Aveugles de France is gratefully acknowledged.

LITERATURE CITED

Albus, K. (1975) A quantitative study of the projection area of the central and visual field in area 17 of the cat. 1. The precision of the topography. Exp. Brain Res. *24:*159–179.

Albus, K., and R. Beckmann (1980) Second and third visual areas of the cat: Interindividual variability in retinotopic arrangement and cortical location. J. Physiol. (Lond.) *299:*247–276.

Allman, J.M., and J.H. Kaas (1974). The organization of the second visual area (VII) in the owl monkey: A second order transformation of the visual hemifield. Brain Res. *76:*247–265.

Barlow, H.B., C. Blakemore, and J.D. Pettigrew (1967) The neural mechanisms of binocular depth discrimination. J. Physiol. *193:*327–342.

Bentivoglio, M., H.G.J.M. Kuypers, C.E. Castman-Berrevoets, H. Loewe, and O. Dann (1980) Two new fluorescent retrograde tracers which are transported over long distance. Neurosci. Lett. *18:*25–30.

Bullier, J., H. Kennedy, and W. Salinger (1984a) Bifurcation of subcortical afferents to visual areas 17, 18 and 19 in the cat cortex. J. Comp. Neurol. *228:*309–328.

Bullier, J., H. Kennedy, and W. Salinger (1984b) Branching and laminar origin of projections between visual cortical areas in the cat. J. Comp. Neurol. *228:*329–341.

Bullier, J., M.E. McCourt, and G.H. Henry (1988) Physiological studies on the feedback connection to the striate cortex from cortical areas 18 and 19 of the cat. Exp. Brain Res. *70:*90–98.

Cleland, B.G., M.W. Dubin, and W.R. Levick (1971) Simultaneous recording of input and output of lateral geniculate neurons. Nature *231:*191–192.

Condé, F. (1987) Further studies on the use of the fluorescent tracers Fast Blue and Diamidino Yellow: Effective uptake area and cellular storage sites. J. Neurosci. Methods *21:*31–43.

Cooper, M.L., and J.D. Pettigrew (1979) A neurophysiological determination of the vertical horopter in the cat and owl. J. Comp. Neurol. *184:*1–26.

Cornwall, J., and O.T. Phillipson (1988) Quantitative analysis of axonal branching using the retrograde transport of fluorescent latex microspheres. J. Neurosci. Methods *24:*1–9.

Cynader, M.S., N.V. Swindale, and J.A. Matsubara (1987) Functional topography in cat area 18. J. Neurosci. *7:*1401–1413.

Deschênes, M., and B. Hu (1990) Electrophysiological and pharmacology of the corticothalamic input to lateral thalamic nuclei: An intracellular study. Eur. J. Neurosci. *2:*140–152.

Donaldson, I.M.L., and D. Whitteridge (1977) The nature of the boundary between cortical visual areas II and III in the cat. Proc. R. Soc. Lond. [Biol.] *199:*445–462.

Douglas, R.J., and K.A.C. Martin (1990) Neocortex. In G.M. Shepherd (ed.): Synaptic Organization of the Brain. New York: Oxford University Press, pp. 220–248.

Dow, B.M., A.Z. Snyder, R.G. Vautin, and R. Bauer (1981) Magnification factor and receptive field size in foveal striate cortex of the monkey. Exp. Brain Res. *44:*213–228.

Dreher, B., A.G. Leventhal, and P.T. Hale (1980) Geniculate input to cat visual cortex: A comparison of area 19 with areas 17 and 18. J. Neurophysiol. *44:*804–825.

Dreher, B., C. Dehay, and J. Bullier (1990) Bihemispheric collateralization of the cortical and subcortical afferents to the rat's visual cortex. Europ. J. Neurosci. *2:*317–331.

Duysens, J., G.A. Orban, H.W. Van der Glas, and F.E. de Zegher (1982) Functional properties of area 19 as compared to area 17 of the cat. Brain Res. *231:*279–291.

Engel, A.K., P. König, C.M. Gray, and W. Singer (1990) Stimulus-dependent neuronal oscillations in cat visual cortex: Intercolumnar interaction as determined by cross-correlation analysis. Eur. J. Neurosci. *2:*588–606.

Ferrer, J.M.R., D.J. Price, and C. Blakemore (1988) The organization of corticocortical projections from area 17 to area 18 of the cat's visual cortex. Proc. R. Soc. Lond. [Biol.] *233:*77–98.

Ferster, D. (1981) A comparison of binocular depth mechanisms in areas 17 and 18 of the cat visual cortex. J. Physiol. *311:*623–655.

Fisken, R.A., L.J. Garey, and T.P.S. Powell (1975) The intrinsic, association and commissural connections of area 17 of the visual cortex. Philos. Trans. R. Soc. [Biol.] *272:*487–536.

Freeman, B., S. Löwel, and W. Singer (1987) Deoxyglucose mapping in the cat visual cortex following artery injection and cortical flat-mounting. J. Neurosci. Methods *20:*115–129.

Gallyas, F. (1979) Silver staining of myelin by means of physical development. Neurol. Res. *1:*203–209.

Gattass, R., A.P.B. Sousa, and E. Covey (1985) Cortical visual areas of the macaque: Possible substrates for pattern recognition mechanisms. In C. Chagas, R. Gattass, and C. Gross (eds.): Pattern Recognition Mechanisms Vol. II. Exp. Brain Res. Suppl., Springer-Verlag, pp. 1–20.

Gattass, R., A.P.B. Sousa, and C. Gross, C. (1988) Visuotopic organization and extent of V3 and V4 of the macaque. J. Neurosci. *8:*1835–1845.

Geisert, E.E. (1980) Cortical projections of the lateral geniculate nucleus in the cat. J. Comp. Neurol. *190:*793–812.

Gilbert, C.D. (1985) Horizontal integration in neocortex. Trends Neurosci. *8:*160–165.

Gilbert, C.D., and J.P. Kelly (1975) The projection of cells in different layers of the cat's visual cortex. J. Comp. Neurol. *163:*81–106.

Gilbert, C.D., and T.N. Wiesel (1989) Columnar specificity of intrinsic horizontal and corticocortical connections in cat visual cortex. J. Neurosci. *9:*2432–2442.

Hammond, P., and D.M. McKay (1975) Differential responses of cat visual cortical cells to textured stimuli. Exp. Brain Res. *22:*427–430.

Henry, G.H., P.A. Salin, and J. Bullier (1991) Projections from area 18 and 19 to cat striate cortex: Divergence and laminar specificity. Eur. J. Neurosci. *3:*186–200.

Hubel, D.H., and T.N. Wiesel (1963) Shape and arrangement of columns in cat's striate cortex. J. Physiol. (Lond.) *165:*559–568.

Hubel, D.H., and T.N. Wiesel (1965) Receptive fields and functional architecture in two nonstriate areas (18 and 19) of the cat. J. Neurophysiol. *28:*229–289.

Hubel, D.H., and T.N. Wiesel (1974) Uniformity of monkey striate cortex: A parallel relationship between field size, scatter and magnification factor. J. Comp. Neurol. *158:*295–305.

Illing, R.B., and H. Wässle (1981) The retinal projections to the thalamus in the cat: A quantitative investigation and a comparison with the retinotectal pathway. J. Comp. Neurol. *202:*265–285.

Jacobs, G.H. (1969) Receptive fields in visual systems. Brain Res. *14:*553–573.

Jones, E.G., H. Burton, and R. Porter (1975) Commissural and corticocortical "columns" in the somatic sensory cortex of primates. Science *190:*572–574.

Kato, H., P.O. Bishop, and G.A. Orban (1978) Hypercomplex and simple/complex cell classification in cat striate cortex. J. Neurophysiol. *41:*1071–1095.

Katz, L.C., A. Burkhalter, and W.J. Dreyer (1984) Fluorescent latex microspheres as a retrograde neuronal marker for in vivo and in vitro studies of visual cortex. Nature *310:*498–500.

Keizer, K., H.G.J.M. Kuypers, A.M. Huisman, and O. Dann (1983) Diamidino Yellow Dihydrochloride (DY.2HCL), a fluorescent retrograde neuronal tracer which migrates only very slowly out the cell and can be used in combinaison with TB and FB in double-labelling experiments. Exp. Brain Res. *512:*179–191.

Kennedy, H., and J. Bullier (1985) A double-labelling investigation of the afferent connectivity of cortical areas V1 and V2 of the macaque monkey. J. Neurosci. *5:*2815–2830.

Kennedy, H., C. Meissirel, and C. Dehay (1991) Callosal pathways in primates and their compliancy to general rules governing the organization of cortico-cortical connectivity. In B. Dreher and S. Robinson (eds.): Neuroanatomy of the Visual Pathways and Their Retinotopic Organisation. Macmillan Press. London.

Kisvarday, Z.F., K.A.C. Martin, F. Freund, Z. Magloczsky, D. Whitteridge, and P. Somogyi (1986) Synaptic targets of HRP-filled layer III pyramidal cells in the cat striate cortex. Exp. Brain Res. *64:*541–552.

LeVay, S. (1988) Patchy intrinsic projections in visual cortex, area 18, of the

cat: Morphological and immunocytochemical evidence for an excitatory function. J. Comp. Neurol. *269*:265–274.

Luhmann, H.J., W. Singer, and L. Martínez-Millán (1990) Horizontal interactions in cat striate cortex: 1. Anatomical substrate and postnatal development. Eur. J. Neurosci. *2*:344–357.

Martin, K.A.C., and D. Whitteridge (1984) Form, function and intracortical projections of spiny neurons in the striate visual cortex of the cat. J. Physiol. *353*:291–302.

Matsubara, J.A., M.S. Cynader, and N.V. Swindale (1987) Antomical properties and physiological correlates of the intrinsic connections in cat area 18. J. Neurosci. *7*:1428–1446.

McIlwain, J.T. (1973) Retinotopic fidelity of striate cortex-superior colliculus interactions in the cat. J. Neurophysiol. *36*:702–710.

McIlwain, J.T. (1977) Topographic organization and convergence in corticotectal projections from areas 17, 18 and 19 in the cat. J. Neurophysiol. *40*:189–198.

Merrill, E.G., and A. Ainsworth (1972) Glass-coated platinum-plated tungsten microelectrodes. Med. Biol. Eng. *10*:662–672.

Mignard, M., and J.G. Malpeli (1991) Patterns of information flow through visual cortex. Science *251*:1249–1251.

Morel, A., and J. Bullier (1990) Anatomical segregation of two cortical visual pathways in the macaque monkey. Vis. Neurosci. *4*:555–578.

Nelson, J.I.N., and B.J. Frost (1978) Orientation selective inhibition from beyond the classic visual receptive field. Brain Res. *139*:359–365.

Nelson, J.I.N., P.A. Salin, M.H.J. Munk, M. Arzi, and J. Bullier (1992) Spatial and temporal coherence in corticocortical connections: A cross-correlation study in areas 17 and 18 in the cat. Vis. Neurosci. *9*:21–38.

Nikara, T., P.O. Bishop, and J.D. Pettigrew (1968) Analysis of retinal correspondence by studying receptive fields of binocular single units in cat striate cortex. Exp. Brain Res. *6*:353–372.

Olavarria, J., and R.C. Van Sluyters (1985) Unfolding and flattening of gyrencephalic brains. J. Neurosci. Methods *15*:191–202.

Orban, G.A. (1984) Neuronal Operations in the Visual Cortex. Studies of Brain Function, Vol. 11. New York: Springer-Verlag.

Orban, G.A., B. Gulyas, and R. Vogels (1987) Influence of moving textured background on direction selectivity of cat striate neurons. J. Neurophysiol. *57*:1792–1812.

Palmer, L.A., A.C. Rosenquist, and R.J. Tusa (1978) The retinotopic organization of lateral suprasylvian areas in the cat. J. Comp. Neurol. *177*:237–256.

Payne, B.R. (1990) The representation of the visual field in the transcallosal sending and receiving zone in cat area 17. Neurosci. Abst. 295.15.

Perkel, D.H., J. Bullier, and H. Kennedy (1986) Topography of the afferent connectivity of area 17 of the macaque monkey: A double labelling study. J. Comp. Neurol. *253*:374–402.

Price, D.J. (1985) Patterns of cytochrome oxidase activity in areas 17, 18 and 19 of the visual cortex of cats and kittens. Exp. Brain Res. *58*:125–133.

Price, D.J. (1986) The postnatal development of clustered intrinsic connections in area 18 of the visual cortex in kitten. Dev. Brain Res. *24*:31–38.

Rockland, K.S., and D.N. Pandya (1979) Laminar origins and terminations of cortical connections of the occipital lobe in the rhesus monkey. Brain Res. *179*:3–20.

Salin, P.A. (1988) Etude de l'organisation topographique des afférents à l'aire striée du chat adulte par une méthode de double marquage. Thèse de Doctorat, Université Cl. Bernard Lyon 1.

Salin, P.A., J. Bullier, and H. Kennedy, H. (1989) Convergence and divergence in the afferent projections to cat area 17. J. Comp. Neurol. *283*:486–512.

Sanides, D., and J. Hoffmann (1969) Cyto- and myelo-architecture of the visual cortex of the cat and the surrounding integration cortices. J. Hirnforsch. *11*:79–104.

Sherk, H., and M. Ombrellaro (1988) The retinotopic match between area 17 and its targets in visual suprasylvian cortex. Exp. Brain Res. *72*:225–236.

Sherman, S.M., and C. Koch (1986) The control of retinogeniculate transmission in mammalian lateral geniculate nucleus. Exp. Brain Res. *63*:1–20.

Sillito, A.M. (1979) Inhibitory mechanisms influencing complex cell orientation selectivity and their modification at high resting discharge levels. J. Physiol. *289*:33–53.

Spear, P.D., and T.P. Baumann (1975) Receptive-field characteristics of single neurons in lateral suprasylvian visual area of the cat. J. Neurophysiol. *38*:1403–1420.

Symonds, L.L., and A.C. Rosenquist (1984) Corticocortical connections among visual areas in the cat. J. Comp. Neurol. *229*:1–38.

Tanaka, K. (1983) Cross-correlation analysis of geniculostriate neuronal relationships in cats. J. Neurophysiol. *49*:1303–1318.

Tigges, J., M. Tigges, and A.A. Perachio (1977) Complementary laminar terminations of afferent to area 17 originating in area 18 and the lateral geniculate nucleus in squirrel monkey. J. Comp. Neurol. *176*:87–100.

Tootell, R.B.H., and M.S. Silverman (1985) Two methods for flat-mounting cortical tissue. J. Neurosci. Methods *15*:177–190.

Ts'o, D.Y., C.D. Gilbert, and T.N. Wiesel (1986) Relationship between horizontal interactions and functional architecture in cat striate cortex as revealed by cross-correlation analysis. J. Neurosci. *6*:1160–1170.

Tusa, R.J., and L.A. Palmer (1980) Retinotopic organization of areas 20 and 21 in the cat. J. Comp. Neurol. *193*:147–164.

Tusa, R.J., L.A. Palmer, and A.C. Rosenquist (1978) The retinotopic organization of area 17 (striate cortex in the cat). J. Comp. Neurol. *177*:213–236.

Tusa, R.J., A.C. Rosenquist, and L.A. Palmer (1979) Retinotopic organization of areas 18 and 19 in the cat. J. Comp. Neurol. *185*:657–678.

Van Essen, D.C., and J.H.R. Maunsell (1980) Two-dimensional maps of the cerebral cortex. J. Comp. Neurol. *191*:255–281.

Van Essen, D.C., and J.H.R. Maunsell (1983) Hierarchical organization and functional streams in the visual cortex. Trends Neurosci. *6*:370–375.

Wong-Riley, M.T.T. (1979a) Changes in the visual system of monoculary sutured or enucleated cats demonstrable with cytochrome oxidase histochemistry. Brain Res. *171*:11–28.

Wong-Riley, M.T.T. (1979b) Columnar cortico-cortical interconnections within the visual system of the squirrel and macaque monkeys. Brain Res. *162*:201–217.